American Journal of Environmental Engineering 2013, 3(4): 147-169
DOI: 10.5923/j.ajee.20130304.01

Turbulent Wind Profiles and Tracer Dispersion for Eolic Park Site Evaluation

K. B. Mello[1,*], B. E. J. Bodmann[2], M. T. Vilhena[2]

[1]Departamento de Ensino, Instituto Federal do Rio Grande do Sul – Câmpus Caxias do Sul, Mario de Boni, 2250, 95012-580. Caxias do Sul, RS, Brazil
[2]P PROMEC & PPGMAp, Universidade Federal do Rio Grande do Sul, Av. Osvaldo Aranha 99/4, 90046-900 Porto Alegre, RS, Brazil

Abstract In this work we discuss stochastic turbulent wind profiles based on the three-dimensional stochastic Langevin equation for a selection of probability density functions and a known mean wind velocity. Its solution permits to simulate tracer dispersion in turbulent regime, which is of interest in evaluating aeolian park sites for wind energy conversion. We discuss the stochastic Langevin equation together with an analytical method for solving the three-dimensional and time dependent equation which is then applied to tracer dispersion for stochastic turbulence models. The solution is obtained using the Adomian Decomposition Method, which provides a direct scheme for solving the problem without the need for linearisation and any transformation. The results of the model are compared to case studies with measured data and compared to procedures and predictions from other approaches.

Keywords Turbulent Wind Profiles, Tracer Disperson, Langevin Equation

1. Introduction

In recent years the Climate Change Problem raised the discussion of limiting and reducing greenhouse gas emissions caused from the burning of fossil fuels, by substitution of these limited resources with renewable and clean energy sources. One promising energy supplier among others is, as sometimes announced, “harnessing the wind”. Although, eolic energy generator technology has left its childhood already some time ago, there are still challenges to be faced in order to restrict or remove certain uncertainties related to this type of electric energy production. The incorporation of eolic energy into the total energy demand still suffers from the fact that supply of wind power depends directly on the wind conditions so that the energy to be injected into the electrical network will be strongly governed by the wind variations but not by the energy demand. In fact, this is the reason why wind energy is said to be unreliable, because of its natural fluctuations. In order to mitigate these difficulties it is of interest to study the wind conditions and its inherent variations on a short term (daily) basis, and a seasonal or long term basis, and turn more predictable the availability of eolic power for a specific site. This knowledge could give support to the management of future wind-park clusters through an additional tool that shall help to minimize or even control the aforementioned variations using probabi-lity based energy distribution plans.

One of the issues addressed in the present article is related to the choice of the site for a possible installation of a wind park considering meteorological aspects as well as possible scenarios simulations and their related experimental validation. One of the possible evaluations of a site candidate may be performed using tracer experiments in order to analyse the wind conditions in the planetary boundary layer, which is typically the layer where eolic turbines are placed. Since this kind of experiments are performed only in a limited set of positions the entire wind velocity field may be reconstructed only by the use of reliable models. However, these models have to be tuned using specific meteorological parameters and conditions in the considered region and shall be subject to the local orography. Furthermore, case studies by model simulations maybe used to establish limits for the generator density using studies with data from already working wind-parks together with model simulations. To this end, existing eolic farms may be used in order to study the influence of generators on changes in the boundary layer wind profile. Such a time sequence analysis may well be performed using tracer experiments, where from the observations one may reconstruct the full space-time wind field by models. This may help to optimise the arrangement of a wind generator cluster taking into account the turbulent structure of the wind field that may in principle be modelled with and without the presence of wind generators. Recent research [11, 38] pointed out the relevance of the mutual wind turbine interaction as well as the impact of the wind flow

* Corresponding author:
kelen.mello@caxias.ifrs.edu.br (K. B. Mello)
Published online at http://journal.sapub.org/ajee

perturbation by turbines on the atmospheric boundary layer in wind farms with extensions beyond the length scale defined by the boundary layer height. In their work the authors quantified the vertical transport kinetic energy and momentum across the boundary layer, which was found to be of the same order of magnitude as the power extracted by the forces that modelled the wind turbines. This finding was directly associated to atmospheric boundary layer turbulence, which is the focus of the present article.

In references[11, 38] a model for the wind energy generators was used to simulate effects on the boundary layer. The present discussion complements the previous works in the sense that one may reconstruct the wind profile with its turbulent properties for the different stability regimes in the planetary boundary layer using data from observations instead of simulating them and tuning the model as to agree reasonably well with the experimental findings. More specifically, the measured average wind velocity field is used (see reference[27]) together with probability density functions, that depend on the stability regime in consideration, and the turbulent contribution is then determined from the nonlinear stochastic Langevin equation. This procedure may be used for analysing potential wind energy park sites or already existing ones. The choice for a Lagrangian model in comparison to an Eulerian approach resides in the fact that the latter yields average values only, whereas Lagrangian models capture the stochastic characteristics of the turbulent wind field by virtue of the employed probability density functions. The mapping of turbulent wind fields instead of mean fields is essential for opening pathways that help increasing the predictability of the wind profile in all stability regimes along the 24 hour cycle, and especially during stability changes. During changes of stability and in the unstable regime, energy of the mean field is transferred to the turbulent field that affects the gain in energy conversion by wind turbines.

In the further we show how the Langevin model is solved analytically using the decomposition method which then may provide short, intermediate and long term (normalized) behaviour and permit to assess the probability of occurrence of higher or lower turbulence levels and additionally serve as a supplement for designing the afore mentioned energy response plans. Note, that natural turbulence is one of the reasons for a decrease of the efficiency of the turbines from its nominal value, and the square ratio of the turbulent velocity to the mean velocity represents a crude measure for that effect. A further aspect worth mentioning is that the average eddy size is roughly of the order of magnitude of the rotor.

The stochastic character of turbulence is implemented using the appropriate Gaussian, bi-Gaussian and Gram - Chalier probability distribution for the different stabilities. Exactness of the solution is manifest in stable convergence, which we control by a Lyapunov theory inspired criterion. The most adequate probability distribution for the wind scenario of interest is indicated by a novel statistical validation index, which from comparison to experimental data selects the most significant model. Comparison to the Copenhagen and to other deterministic approaches shows the advantage of the present analytical approach even for considerably rugged land relieves.

Our article is organised as follows. In section 2 we report on the state of the art of stochastic wind profile modelling, and show how a closed form solution may be obtained by Adomian's decomposition method. In 3, we present the numerical results for three probability density functions and in section 4 we come to our conclusions.

2. Stochastic Wind Profile Modelling

Atmospheric turbulence and tracer dispersion in the planetary boundary layer is a stochastic process and thus obeys a stochastic law which may be expressed as a set of stochastic differential equations. For a time dependent regime considered in the present work, we assume that the associated Langevin equation adequately describes atmospheric turbulence and dispersion processes, which we test by comparison to other methods in order to pin down computational errors and finally analyse for model adequacy. We are aware of the fact that up to date there do exist a variety of models and approaches to the problem, either based on numerical schemes, stochastic simulations or (semi-) analytical approaches and indicate in the further a selection of models. Numerical approaches may be found in the works of Tangerman[45], Brebbia[8], Chock et al.[17], Sharan et al.[41] and Huebner et al.[31]. There are various models that have been used effectively in the past to describe tracer dispersion[48],[42],[6],[5], and many of them make use of analytical approaches[35, 42, 43]. One also finds semi-analytical methods, where we mention the works of Parlange[39], Dike[20], Henry et al.[29], Grisogono and Oerlemans[25], Metha and Yadav[37], Carvalho et al.[13] and Carvalho and Vilhena[12].

Upon developing a model one typically faces various problems. First one has to identify a differential equation that shall represent a model or a physical law. Once the law/model is accepted as the fundamental equation one challenges the task of solving the equation in many cases approximately and analyse the error of approximation and numerical errors in order to validate its prediction against experimental data. Experimental data of a stochastic process typically spread around average values, i.e. are distributed according to probability distributions. Hence, the model shall within certain limits reproduce the experimental findings. Since the fundamental equation is already a simplification deviations may occur which in general have their origin in a model error superimposed by numerical or approximation based errors. In case of a genuine convergence criterion one may pin down the error analysis essentially to a model validation. Since in general convergence is handled by heuristic convergence criteria, a model validation is not that obvious. Thus we show with the present discussion, that our semi-analytical approach does

not only yield an acceptable solution to the Langevin equation but predicts tracer concentrations closer to observed values than predictions from other models values with is also manifest in the statistical analysis.

Simulation of tracer dispersion in the Planetary Boundary Layer (PBL) through a Lagrangian particle model by the use of the Langevin equation and its diffusion equation limit (random displacement equation) usually has been solved by the method of Ito calculus[24, 40]. More recently one of the authors developed the Iterative Langevin Solution (ILS) method, which solves the Langevin equation in a semi-analytical manner by the method of successive approximations, known as Picard's iterative method. The method is principally characterised by the following steps: Application of Picard's procedure on the Langevin equation, to be more specific, integration, linearisation of the stochastic non-linear term and iterative solution of the resultant equation, which permits to evaluate an analytical expression for the velocity. Details of this approach may be found elsewhere[13, 14, 12, 44, 15, 16].

An alternative analytical method for solving linear and non-linear differential equations was developed by Adomian[1], known as the decomposition method. The decomposition procedure permits to cast the solution into a convergent series by using the necessary number of recursions for both linear and non-linear deterministic and stochastic equations. The advantage of this method is that it provides a direct scheme for solving the problem without the need for linearisation or transformations. There exists a vast literature about applications of this method to a broad class of physical problems and we cite the works we considered relevant for the further discussion[1, 2, 3, 22, 34, 32, 19, 21]. Thus the present work extends the list of methods that solve the Langevin equation assuming Gaussian, bi-Gaussian and Gram-Chalier turbulence condition by Adomian's approach. The variety of methods, such as the numerical solution of the Langevin equation (integrated according to the Ito calculus), analytical solution of the Langevin equation (derivation of Uhlenbeck and Ornstein[47]), Iterative Langevin Solution (ILS) and solution by decomposition (ADM)[26].

2.1. The Decomposition Method for a Stochastic Process

A time dependent stochastic process μ is typically characterized by its time evolution, which depends on stochastic contributions, such as expectation values (E_n) of mean field character (E_0) and higher moments (here E_2), respectively. In our case we consider the Langevin equation to describe turbulence.

$$\mu(t+\tau)-\mu(t)=\int_t^{t+\tau}E_0(\mu(t'),t')dt'+\int_t^{t+\tau}E_2(\mu(t'),t')^{\frac{1}{2}}d\Sigma(t') \tag{1}$$

Here $d\Sigma$ is a stochastic measure for random motion and E_0 represents a drift like term, whereas E_2 is a measure for diffusion intensity, which satisfy the usual Lipschitz continuity condition in order to ensure the existence of a unique strong solution. In case of a Wiener process $\mu(t)$ is Markovian, but in our case we presume that the process is an Ito process, i.e. it depends on the present and previous values, hence the integral form of mean field and fluctuation contributions. Note, that the integral form will be used further down in order to set-up the solution following Adomian's prescription, which we resume in the following.

One may rewrite the stochastic equation from above (1) as a differential equation, upon using the limit $\tau\to 0$ and separating all terms depending on the process μ including the differential operator (LHS of equation(2)) from the noise generating term $G(t)$ (the stochastic contribution, last term in eq. (1)).

$$L[\mu(t)]=L_L[\mu(t)]+L_N[\mu(t)]=G(t) \tag{2}$$

According to Adomian, one splits the linear operator, that includes the derivatives L_L with known inversion from the non-linear terms L_N. Further we write $\mu(t)$ as a sum of a convergent sequence $\mu_i(t)$, still to be specified, and the nonlinear term is cast into a sum of so called Adomian functional polynomials[1].

$$\mu(t)=\sum_{i=0}^{\infty}\mu_i(t) \qquad L_N[\mu]=\sum_{i=0}^{\infty}A_i \tag{3}$$

For the nonlinear part we use a normal convergent operator expansion

$$\frac{\partial^m}{\partial\mu^m}\left(L_N[\mu]\right)=\frac{\partial^m F}{\partial\mu^m}=F^{(m)} \tag{4}$$

and rewrite the non-linear term as

$$L_N[\mu]=\sum_{n=0}^{\infty}\frac{1}{n!}\underbrace{\frac{\partial^n F}{\partial\mu^n}\bigg|_{\mu=\mu_0}}_{F_0^{(n)}}\left(\sum_{m=1}^{\infty}\mu_m\right)^n=\lim_{r\to\infty}\sum_{n=0}^{\infty}\frac{1}{n!}F_0^{(n)}\sum_{\substack{k_1,\ldots,k_r\\ \sum k_i=n}}\left(\binom{n}{\{k_i\}_1^r}\prod_{m=1}^{r}\mu_m^{k_m}\right)$$

$$=F_0^{(0)}+\sum_{n=1}^{\infty}\left(F_0^{(1)}\mu_n+\sum_{j=2}^{\infty}\frac{1}{j!}F_0^{(j)}\sum_{\substack{k_1,\ldots,k_{n-1}\\ \sum k_i=j}}\left(\binom{j}{\{k_i\}_1^{n-}}\prod_{m=1}^{n-1}\mu_m^{k_m}\right)\right) \tag{5}$$

where we introduced the shorthand notations for the derivative terms $F_0^{(n)}$ the polynomial coefficients $\binom{n}{\{k_i\}_1^r} = \binom{n}{k_1,\ldots,k_r}$. Introducing these terms into the original differential equation permits to identify corresponding terms, that give rise to the iterative scheme in the spirit of Adomian as shown next.

$$\sum_{n=1}^{\infty} L_L\left[\mu_i(t)\right] = G(t) - F_0^{(0)} - \\ +\sum_{n=1}^{\infty}\left(F_0^{(1)}\mu_n + \sum_{j=2}^{\infty}\frac{1}{j!}F_0^{(j)} \sum_{\substack{k_1,\ldots,k_{n-1} \\ \sum k_i = j}} \left(\binom{j}{\{k_i\}_1^{n-}} \prod_{m=1}^{n-1} \mu_m^{k_m} \right) \right) \quad (6)$$

There are many possibilities to setup an iterative scheme which upon truncation to n terms in A_n and $n + 1$ terms in μ_n yields an approximate solution in analytical form. Instead of solving the original Langevin equation we cast the problem into a set of simpler equations which may be solved because the integral operator L_L^{-1} is known.

$$L_L[\mu_0] = G$$
$$L_L[\mu_1] = -A_0 = -F_0^{(0)}$$
$$L_L[\mu_2] = -A_1 = -F_1^{(0)}\mu_1$$
$$L_L[\mu_2] = -A_1 = -F_1^{(0)}\mu_2 - \frac{1}{2}F_0^{(1)}\mu_1^2 \quad (7)$$
$$L_L[\mu_{n+1}] = -A_n = \\ -\sum_{n=1}^{\infty}\left(F_0^{(1)}\mu_n + \sum_{j=2}^{\infty}\frac{1}{j!}F_0^{(j)} \sum_{\substack{k_1,\ldots,k_{n-1} \\ \sum k_i = j}} \left(\binom{j}{\{k_i\}_1^{n-}} \prod_{m=1}^{n-1} \mu_m^{k_m} \right) \right)$$

The way we have setup the iterative scheme defines the seed $\mu_0(t)$ by the stochastic contribution as source term, whereas the remaining iterators are simply given by the Adomian functional polynomials as source terms of the equations to be solved. Note that in order to evaluate the i-th recursion step μ_i the μ_j with $j < i$ are known from the previous iteration steps. Moreover, the functional expansion of the non-linear term around the function μ_0 shows how the stochastic term effectively enters in the remaining terms μ_i with $i > 0$ from the non-linearity.

2.2. A Convergent Closed Form Solution

The iteration defines a convergent series towards μ for all t in a certain domain, thus the solution $\mu = \lim_{n\to\infty}\sum_{i=0}^{n}\mu_i$ is manifest exact. Since this scheme defines an explicit analytical expressions for the μ_i and A_i, respectively, one arrives at a procedure which permits to solve the differential equation without linearisation in closed form. The procedure has been applied to a variety of nonlinear problems but an analytical procedure for testing convergence to the best of our knowledge has not been presented in literature, only numerical schemes may be found, see for instance refs.[32] and[4].

In general convergence is not guaranteed by the decomposition method, so that the solution shall be tested by a convenient criterion. Since standard convergence criteria do not apply for the present case due to the non-linearity and stochastic character, we present a method which is based on the reasoning of Lyapunov[9]. While Lyapunov introduced this conception in order to test the influence of variations of the initial condition on the solution, we use a similar procedure to test the stability of convergence while starting from an approximate (initial) solution μ0 (the seed of the iteration scheme).

Let us denote $|\delta Z_n| = \left\|\sum_{i=n+1}^{\infty}\mu_i\right\|$ the maximum deviation of the correct from the approximate solution $\Gamma_n = \sum_{i=0}^{n}\mu_i$, where $\|\cdot\|$ signifies the maximum norm. Then convergence occurs if there exists an n_0 such that the sign of λ is negative for all $n \geq n_0$.

$$\lambda = \frac{1}{\|\Gamma_n\|}\log\left(\frac{|\delta Z_n|}{|\delta Z_0|}\right) \quad (8)$$

In the further we apply the decomposition method as presented in general form above to the problem of tracer dispersion for three different turbulence probability density functions, i.e. Gaussian, bi-Gaussian and Gram-Chalier, respectively. The analysis of convergence is applied to all cases that shows that for $n_0 = 4$ the approach is convergent with an error less than 1%.

3. The Langevin Equation for Stochastic Turbulence

The stochastic equation (1) may be interpreted in terms of the Langevin equation, where μ represents the turbulent velocity vector with components u_i. In the Langevin equation[40] the time evolution of the turbulent velocity is driven by a dissipative term and a second term which may be understood as the gradient of a potential that depends on the fluctuations of the turbulent velocity and represents a mean field interaction of the tracer with the environment it is immersed. The last term represents the stochastic contribution due to a continuous series of particle collisions. All paragraphs must be indented.

$$\frac{du_i}{dt} + \alpha_i u_i = \beta_i + \gamma_i u_i^2 + (C_o\varepsilon_i)^{\frac{1}{2}}\xi_i(t). \quad (9)$$

Here u_i with $i = 1, 2, 3$ is a Cartesian component of the turbulent velocity, which is related to the infinitesimal displacement and the wind velocity U_i by $dx_i = (U_i + u_i)dt$. The coefficients α_i, β_i, γ_i of eq. (9) depend on the employed probability density function. Here C_0 is the Kolmogorov constant, ε is the rate of turbulence kinetic energy dissipation, and ξ_i is a random increment according to a probability density function.

Upon application of the described decomposition method from above (see 2.1) on equation (9), the turbulent velocity is decomposed into a series and the non-linear contribution is taken care of by Adomian's procedure.

$$\frac{d}{dt}\left(\sum_{n=0}^{\infty} u_i,n\right)+\alpha_i\left(\sum_{n=0}^{\infty} u_i,n\right)=\beta_i + (C_o\varepsilon_i)^{\frac{1}{2}}\xi_i(t)+\gamma_i\left(\sum_{n=0}^{\infty} A_{i,n}\right), \quad (10)$$

where the non-linear term is $\sum_{n=0}^{\infty} A_{i,n}=u_i^2$.

Table 1. Meteorological parameters measured during the Copenhagen experiment. L is the Monin-Obukohv length, z_i the convective boundary layer height, u_* is the local friction velocity, w_* is the convective velocity scale, *U(10)* is the wind speed in 10 m and *U(115)* is the wind speed in 115m and h is the PBL height

Run	L (m)	Zi=h (m)	u_* (m/s)	w_* (m/s)	U(10) (m/s)	U(115) (m/s)
1	-37	1980	0.36	1.8	2.1	3.4
2	-292	1920	0.73	1.8	4.9	10.6
3	-71	1120	0.38	1.3	2.4	5.0
4	-133	390	0.38	0.7	2.5	4.6
5	-444	820	0.45	0.7	3.1	6.7
6	-432	1300	1.05	2.0	7.2	13.2
7	-104	1850	0.64	2.2	4.1	7.6
8	-56	810	0.69	2.2	4.2	9.4
9	-289	2090	0.75	1.9	5.1	10.5

In the iterative scheme the stochastic component is absorbed in the first term u_0 of the expansion and thus propagates through all subsequent terms, whereas the nonlinear (mean field) term enters as a correction from the second term on. For any given truncation m the solution for the considered problem (9) is given in closed analytical form summing up the terms $\sum_{n=0}^{m} u_{i,n}$.

So far we have not defined the probability density function, that characterizes the type of turbulence which is correlated to the stability of the planetary boundary layer (PBL). In the studies of turbulent dispersion the stochastic behaviour maybe classified according to stationarity or non-stationarity, according to spatial properties as homogeneity or non-homogeneity and according to the profile of the wind distribution, as Gaussian or non-Gaussian. When employing Lagrangian models one usually considers stationary and homogeneous turbulence in horizontal sheets and non-homogeneous and either Gaussian or non-Gaussian in the vertical direction depending on the stability condition. In stable or neutral conditions the velocity distribution may be considered Gaussian, whereas during convective conditions the velocity distribution is non-Gaussian because of the skewness of the turbulent velocity distribution, which has its origin in up-and down-drafts with different intensity. In the following we present the solutions for the three afore mentioned probability density functions together with their model validation against the data from the Copenhagen experiment[26].

3.1. The Copenhagen Experiment

The Copenhagen tracer experiment[26] was carried out in the northern part of Copenhagen. A tracer (SF6) was released without buoyancy from a tower at a height of 115m and collected at the ground-level positions in up to three crosswind arcs of tracer sampling units. The sampling units were positioned 2km-6km from the point of release. A total of nine tracer experiment runs were performed with instability conditions as shown in table 1. The site was mainly residential with a roughness length of 0.6m. Wind speeds at 10 and 115 meters were used to calculate the coefficient for the vertical exponential wind profile, which is used to model the wind speed.

$$\chi=\left[\frac{\log\left(\frac{U(115)}{U(10)}\right)}{\log\left(\frac{115}{10}\right)}\right], \qquad U(z)=U(0)\left[\frac{z}{10}\right]^{\chi} \quad (11)$$

where U(10) is the wind speed in 10m and U(115) is the wind speed in 115m, respectively.

For the simulations, the turbulent flow is assumed inhomogeneous only in the vertical direction and the transport is realized by the longitudinal component of the mean wind velocity. The horizontal domain was determined according to sampler distances and the vertical domain was set equal to the observed PBL height. The time step was maintained constant and was obtained according to the value of the Lagrangian decorrelation time scale ($\Delta t = \tau_L/c$), where τ_L must be the smaller value among τ_{Lu}, τ_{Lv}, τ_{Lw} and C is an empirical coefficient set equal to 10. In Equation (10), the product $C_0\varepsilon$ is calculated in terms of the turbulent velocity variance σ_i^2 and the Lagrangian decorrelation time scale τ_{Li}[30, 46], which are parametrised according to a scheme developed by Degrazia et al. ([18]). These parametrisations are based on Taylor's statistical diffusion theory and the observed spectral properties. The concentration field is determined by counting the particles in a cell or imaginary volume in the position x, y, z. The integration eq. (10) was computed by the Romberg method.

3.2. Solution for Gaussian Turbulence

In the case where a Gaussian probability density function describes best the stochastic turbulence the coefficients of the Langevin equation (9) and (10) are

$$\alpha_i=\frac{C_0\varepsilon}{2\sigma_i^2}, \beta_i=\frac{1}{2}\frac{\partial\sigma_i^2}{\partial x_j}, \gamma_i=\frac{1}{2\sigma_i^2}\left(\frac{\partial\sigma_i^2}{\partial x_j}\right). \quad (12)$$

In Table (2) we compare the experimental findings with the model predictions by the proposed procedure (ADM – Adomian Decomposition Method), by the Ito method[40], by the ILS method[12] and the early analytical derivation (ANA) by Uhlenbeck and Ornstein[47]. From the comparison one observes a reasonable agreement among the

models and also with the experimental data. In the following table the numerical convergence of the ADM approach for a Gaussian probability density function (pdf) is indicated. The convergence analysis shows that already a few terms represent an analytical solution with spurious error only. The figures 1 show the Lyapunov exponent of the Adomian approach depending on the number of terms for the 9 experimental runs. Note, that the more negative the exponent λ the more stable is convergence. Figure (2) shows the dispersion of the Copenhagen experimental data in comparison with their model predictions by ADM, Ito, ILS, ANA. Note, that the closer the data are grouped to the bisector the better is the agreement between experiment and prediction.

Table 2. Concentrations of nine runs with various positions of the Copenhagen experiment and model prediction by the approaches ADM, ILS, Ito and ANA, using a Gaussian probability density function

Exp.	Distance (m)	Observed (μgm^{-2})	Predictions Cy (μgm^{-2})			
			ADM	ILS	Ito	ANA
1	1900	2074	2092	2770	1486	2320
1	3700	739	1281	725	1001	2046
2	2100	1722	496	1699	1344	1290
2	4200	944	850	1489	1117	1059
3	1900	2624	2601	2710	1649	2366
3	3700	1990	1605	2136	1073	2066
3	5400	1376	1273	1328	1947	2062
4	4000	2682	2379	2726	1947	1565
5	2100	2150	2586	2138	2042	2090
5	4200	1869	1818	2484	1967	1701
5	6100	1590	1568	2206	1690	1819
6	2000	1228	951	915	872	853
6	4200	688	619	775	718	651
6	5900	567	488	673	612	622
7	2000	1608	1172	1606	1015	1320
7	4100	780	680	1290	660	1145
7	5300	535	554	933	548	1170
8	1900	1248	1228	1252	1099	726
8	3600	606	723	522	887	667
8	5300	456	489	416	737	682
9	2100	1511	1433	1660	1330	1334
9	4200	1026	884	1135	1162	1068
9	6000	855	630	894	962	1115

Table 3. Numerical Convergence of ADM using a Gaussian pdf. The multiple columns for Cy refer to the measurements at different distances per run and are given in table 2

Run	Terms	Cy (μgm^{-2})		
1	u_0	2063.595	1289.481	
	$u_0 + u_1$	2010.773	1340.828	
	$u_0 + u_1 + u_2$	2011.426	1308.431	
	$u_0 + u_1 + u_2 + u_3$	2092.073	1281.515	
	$u_0 + u_1 + u_2 + u_3 + u_4$	2092.073	1281.515	
2	u_0	1417.238	823.5428	
	$u_0 + u_1$	1356.679	855.5662	
	$u_0 + u_1 + u_2$	1495.957	850.2274	
	$u_0 + u_1 + u_2 + u_3$	1495.957	850.2274	
	$u_0 + u_1 + u_2 + u_3 + u_4$	1495.957	850.2274	
3	u_0	2549.781	1563.213	1292.831
	$u_0 + u_1$	2615.559	1607.727	1250.595
	$u_0 + u_1 + u_2$	2600.684	1526.362	1253.927
	$u_0 + u_1 + u_2 + u_3$	2601.178	1604.603	1272.520
	$u_0 + u_1 + u_2 + u_3 + u_4$	2601.178	1604.603	1272.520
4	u_0	2376.284		
	$u_0 + u_1$	2444.419		
	$u_0 + u_1 + u_2$	2427.065		
	$u_0 + u_1 + u_2 + u_3$	2379.459		
	$u_0 + u_1 + u_2 + u_3 + u_4$	2379.459		
5	u_0	2134.523	1525.608	1454.858
	$u_0 + u_1$	2215.876	1523.247	1491.563
	$u_0 + u_1 + u_2$	2544.441	1794.193	1626.543
	$u_0 + u_1 + u_2 + u_3$	2586.452	1817.632	1567.856
	$u_0 + u_1 + u_2 + u_3 + u_4$	2586.452	1817.632	1567.856
6	u_0	959.1522	567.4748	471.1268
	$u_0 + u_1$	912.4229	619.4894	518.6852
	$u_0 + u_1 + u_2$	890.4201	605.0680	454.2511
	$u_0 + u_1 + u_2 + u_3$	942.7131	620.3289	483.5103
	$u_0 + u_1 + u_2 + u_3 + u_4$	951.0098	619.3738	488.264
	$u_0 + u_1 + u_2 + u_3 + u_4 + u_5$	951.0098	619.3738	488.264
7	u_0	1087.322	699.6638	585.6924
	$u_0 + u_1$	1122.203	687.8445	624.9547
	$u_0 + u_1 + u_2$	1098.108	682.8063	537.3536
	$u_0 + u_1 + u_2 + u_3$	1171.588	679.6330	554.0372
	$u_0 + u_1 + u_2 + u_3 + u_4$	1171.588	679.6330	554.0372
8	u_0	1184.016	787.5058	489.2957
	$u_0 + u_1$	1150.614	780.2734	502.6539
	$u_0 + u_1 + u_2$	1228.163	722.6319	489.3400
	$u_0 + u_1 + u_2 + u_3$	1228.163	722.6319	489.3400
	$u_0 + u_1 + u_2 + u_3 + u_4$	1228.163	722.6319	489.3400
9	u_0	1404.454	853.9096	679.9700
	$u_0 + u_1$	1332.897	825.2356	681.6997
	$u_0 + u_1 + u_2$	1523.163	876.8478	661.7837
	$u_0 + u_1 + u_2 + u_3$	1433.129	884.0126	630.3093
	$u_0 + u_1 + u_2 + u_3 + u_4$	1433.129	884.0126	630.3093

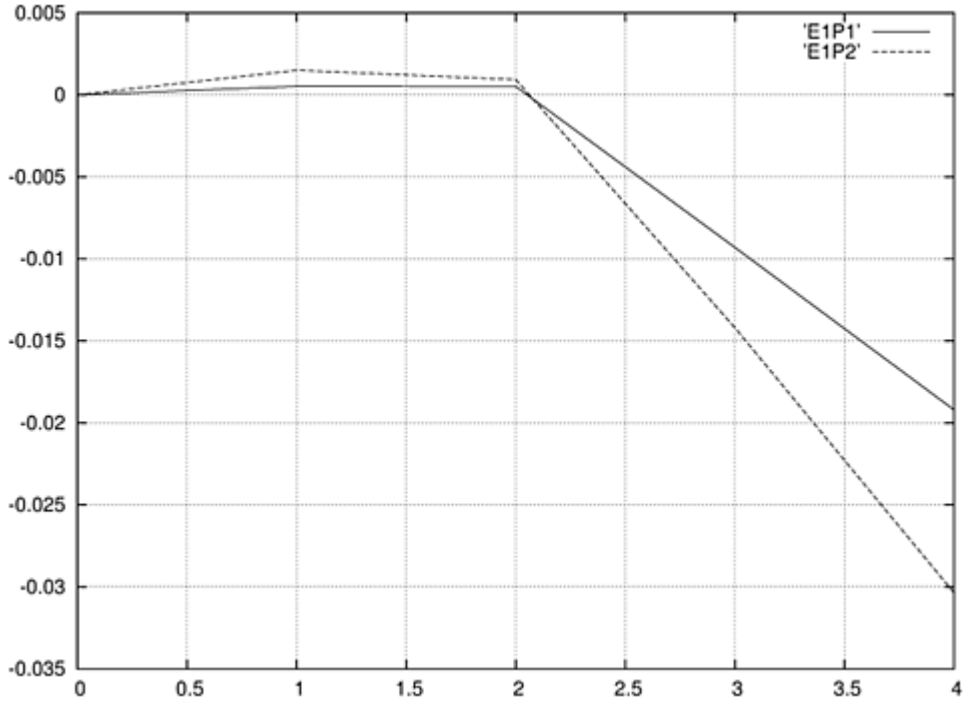
'E1P1'
'E1P2'
0.005
0
-0.005
-0.01
-0.015
-0.02
-0.025
-0.03
-0.035
0
0.5
1
1.5
2
2.5
3
3.5
4

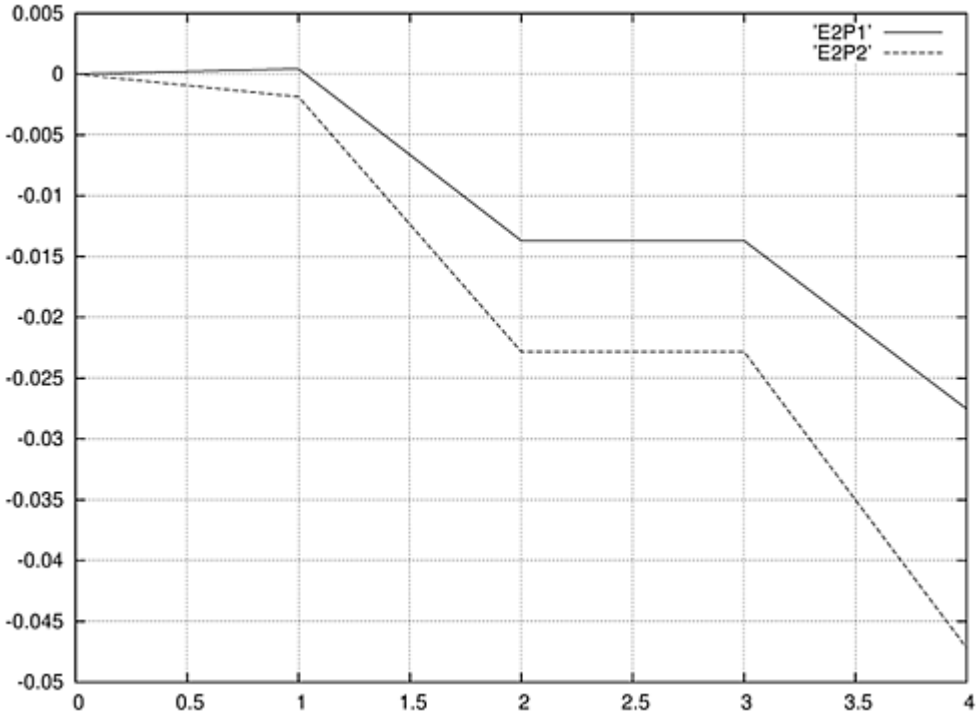
'E2P1'
'E2P2'
0.005
0
-0.005
-0.01
-0.015
-0.02
-0.025
-0.03
-0.035
-0.04
-0.045
-0.05
0
0.5
1
1.5
2
2.5
3
3.5
4

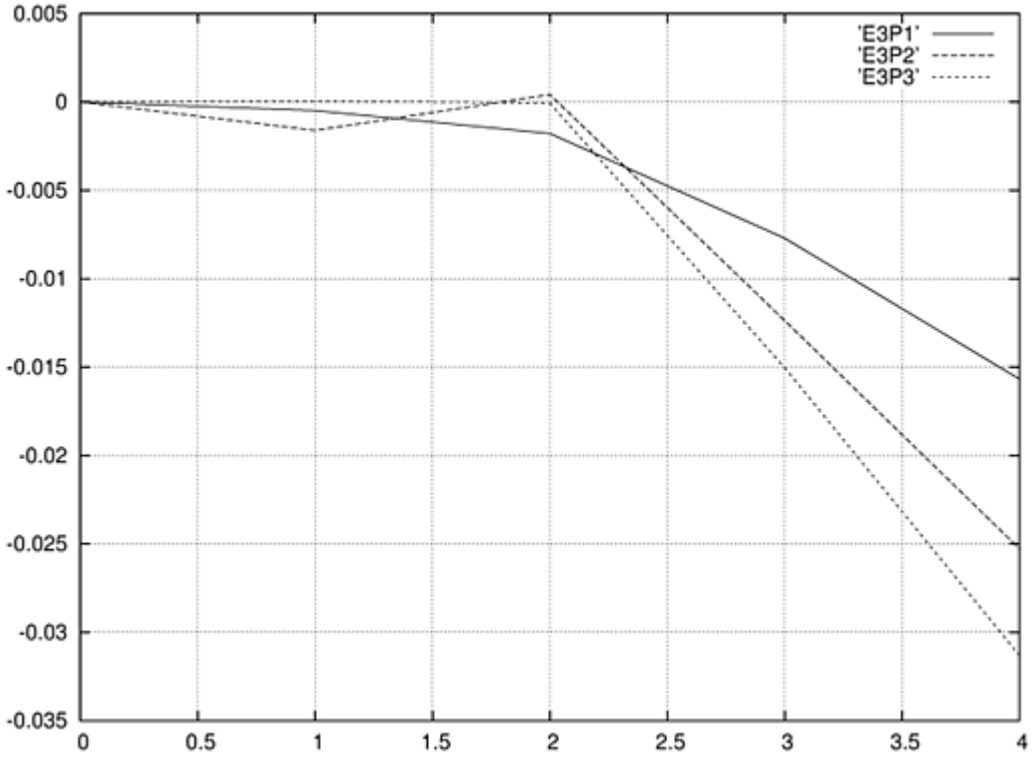
'E3P1'
'E3P2'
'E3P3'
0.005
0
-0.005
-0.01
-0.015
-0.02
-0.025
-0.03
-0.035
0
0.5
1
1.5
2
2.5
3
3.5
4

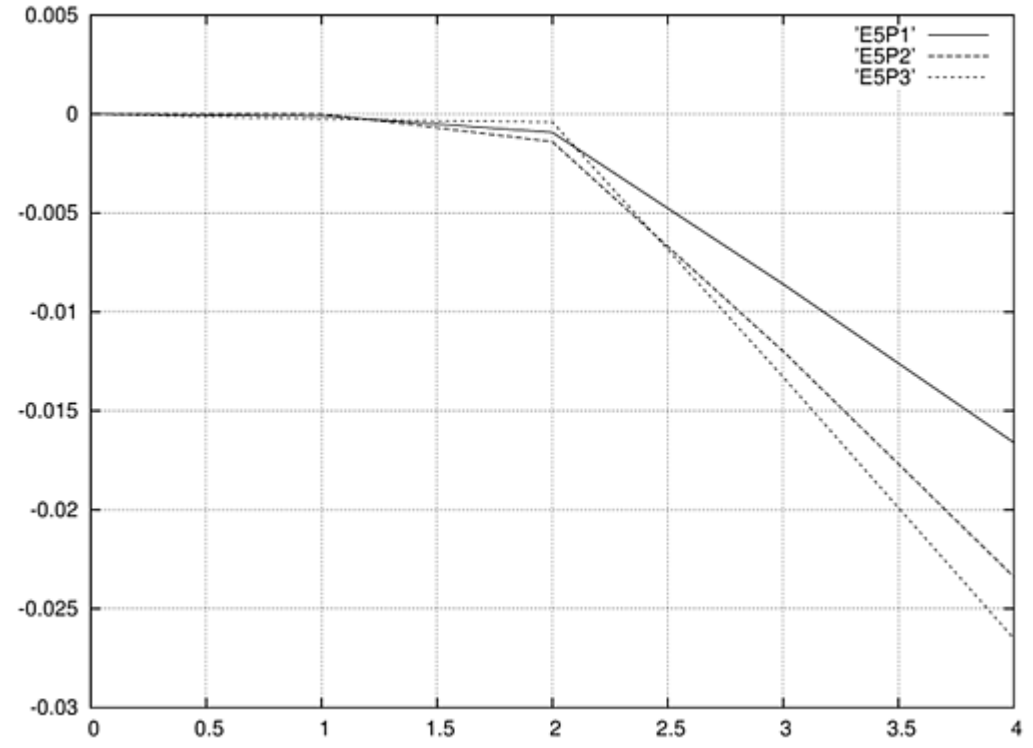
'E5P1'
'E5P2'
'E5P3'
0.005
0
-0.005
-0.01
-0.015
-0.02
-0.025
-0.03
0
0.5
1
1.5
2
2.5
3
3.5
4

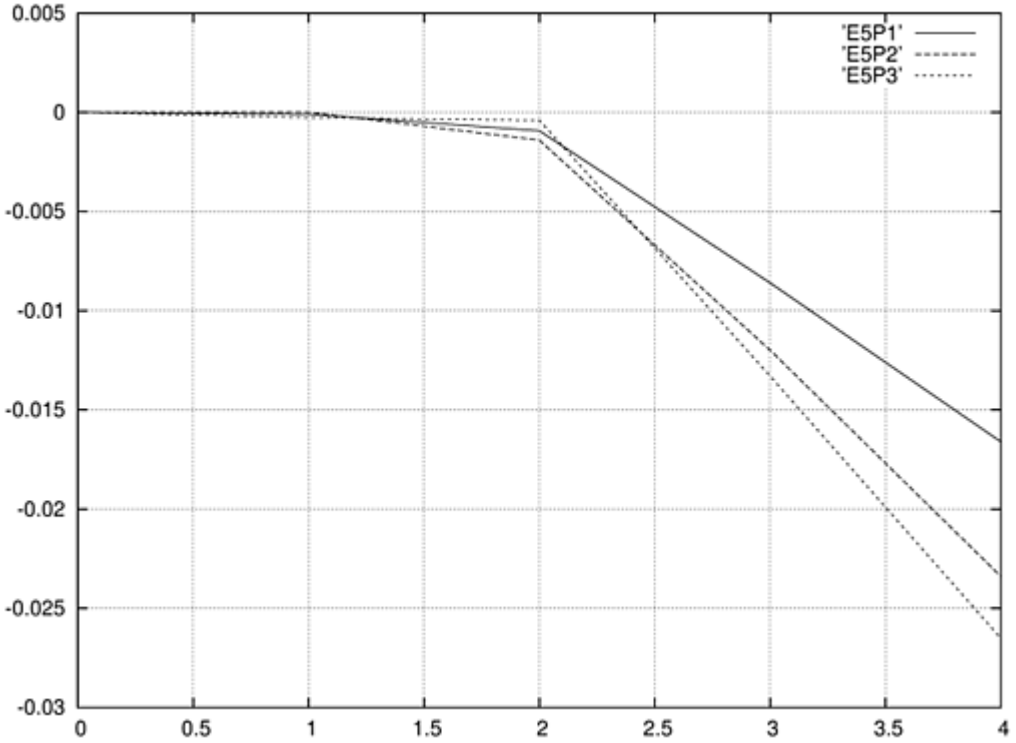
'E5P1'
'E5P2'
'E5P3'
0.005
0
-0.005
-0.01
-0.015
-0.02
-0.025
-0.03
0
0.5
1
1.5
2
2.5
3
3.5
4

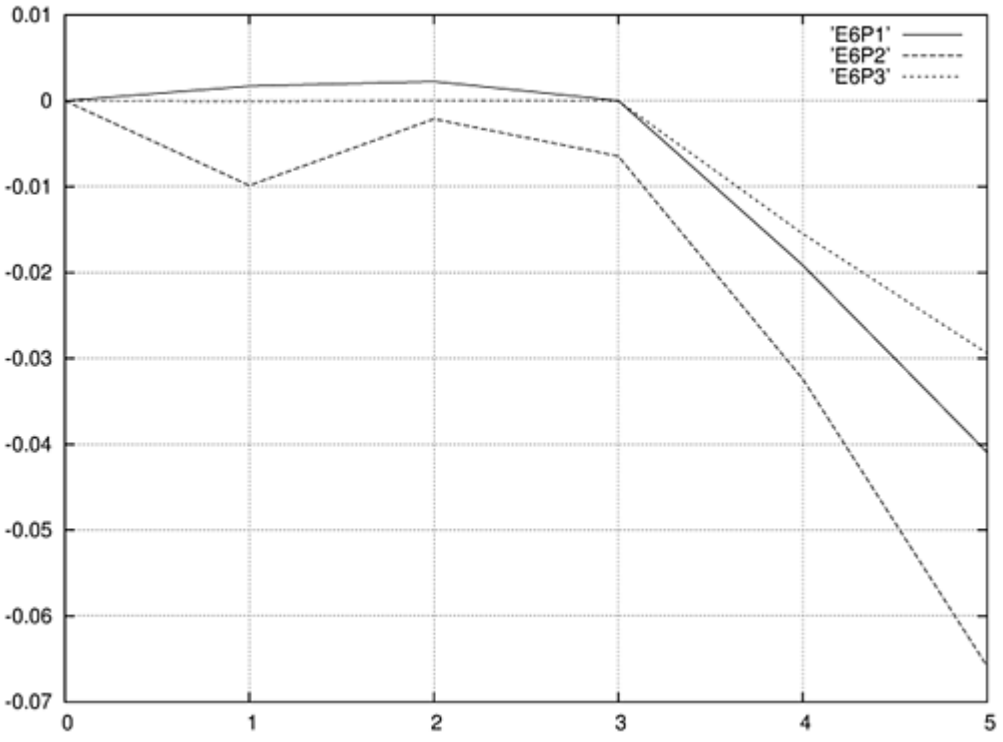
'E6P1'
'E6P2'
'E6P3'
0.01
0
-0.01
-0.02
-0.03
-0.04
-0.05
-0.06
-0.07
0
1
2
3
4
5

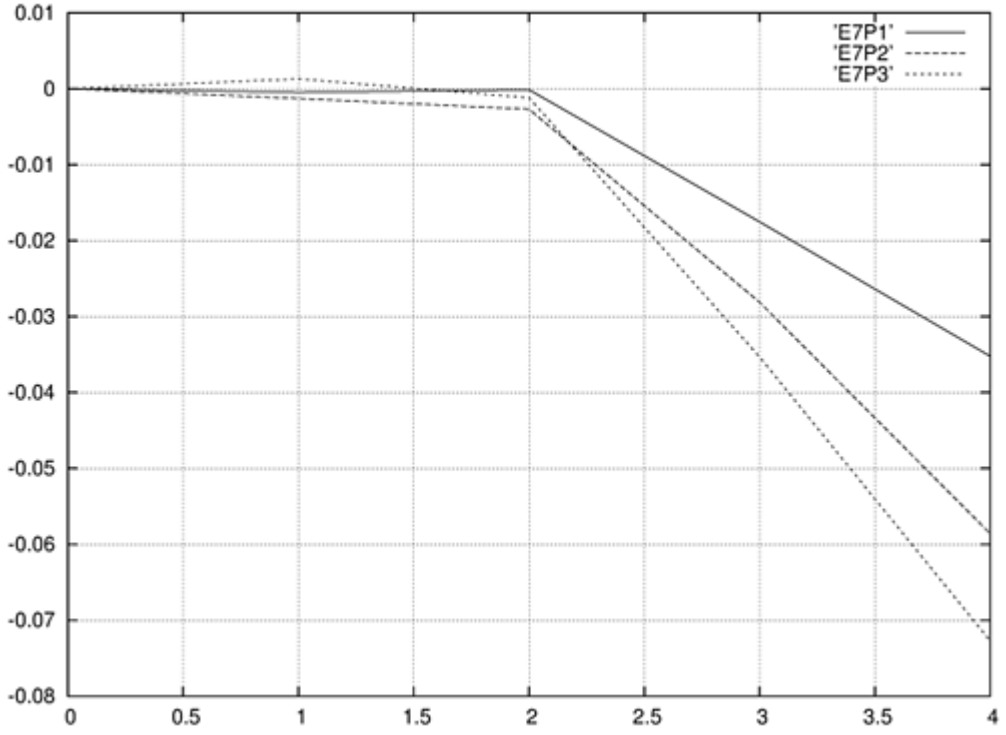
'E7P1'
'E7P2'
'E7P3'
0.01
0
-0.01
-0.02
-0.03
-0.04
-0.05
-0.06
-0.07
-0.08
0
0.5
1
1.5
2
2.5
3
3.5
4

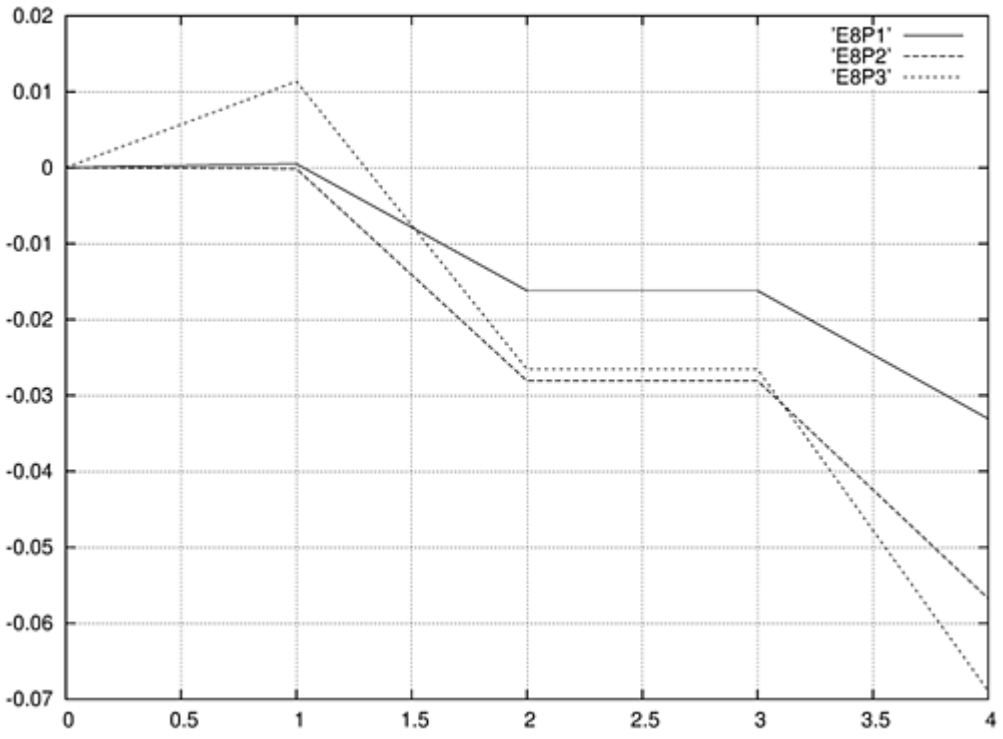
'E8P1'
'E8P2'
'E8P3'
0.02
0.01
0
-0.01
-0.02
-0.03
-0.04
-0.05
-0.06
-0.07
0
0.5
1
1.5
2
2.5
3
3.5
4

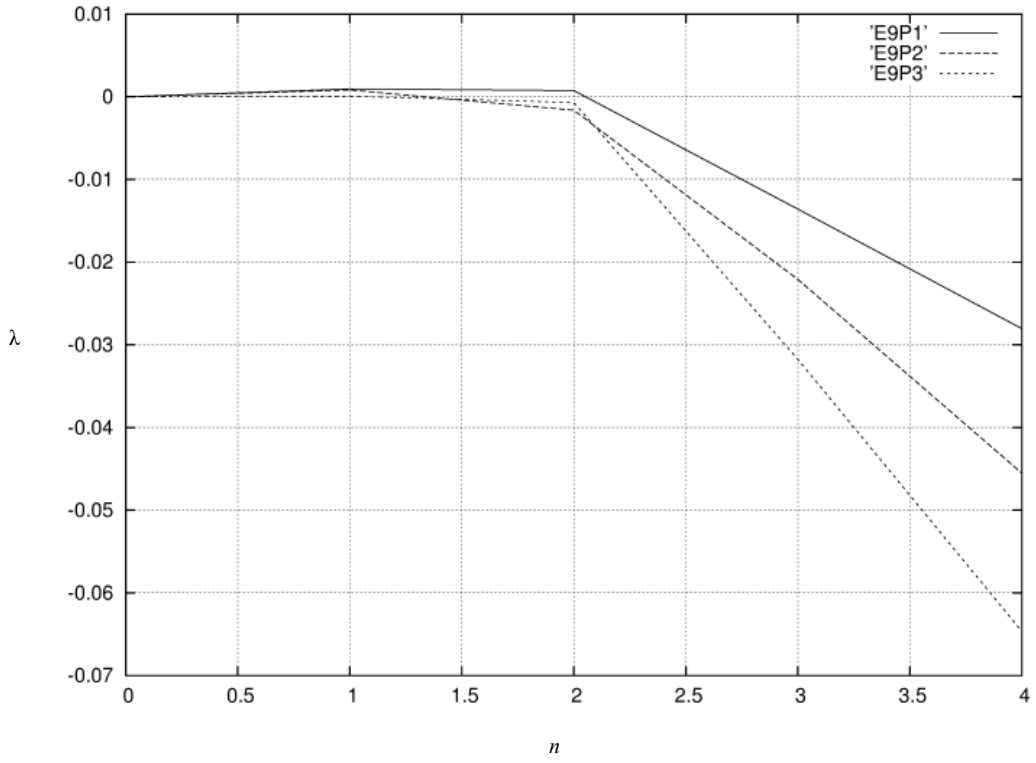

Figure 1. Lyapunov exponent λ of Adomian approach depending on the number n of terms for the 9 experiment runs

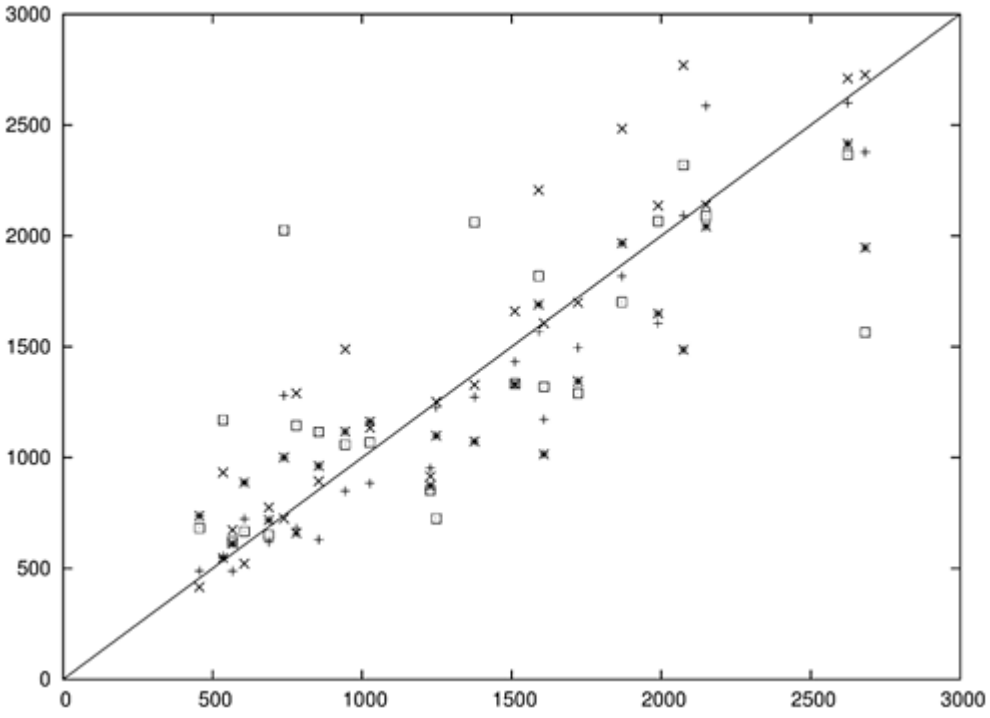

Figure 2. Dispersion diagram of predicted (C_p) measured against measured (C_o) values by by ADM (+), ILS (×) , Ito (*) e ANA (□)

In figure 3 we show the linear regression of each model, where the closer their intersect is to the origin and the closer the slope is to unity the better is the approach. By comparison one observes that the present approach yields the best description of the data. Details of the regression may be found in table 4.

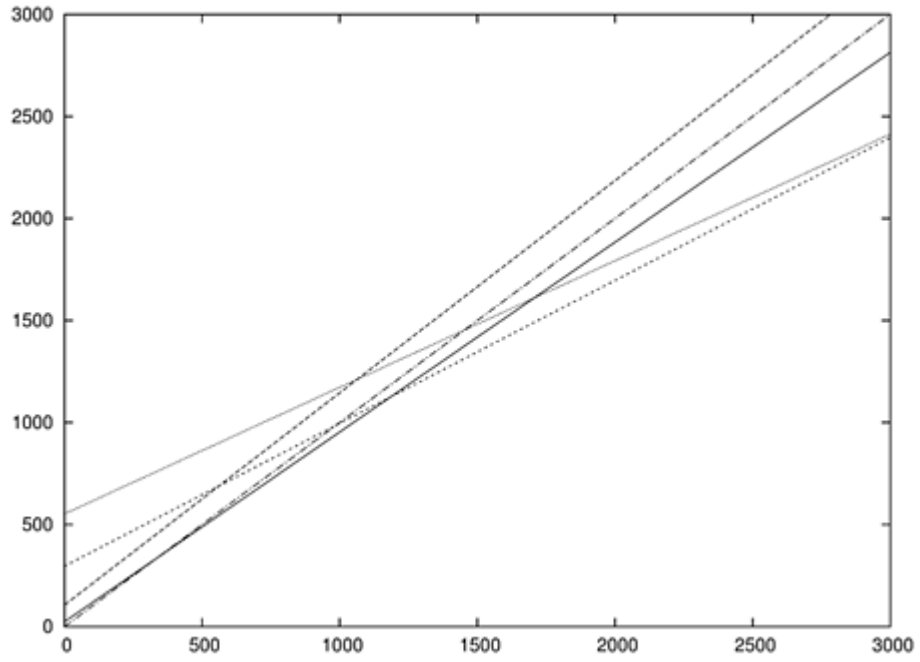

Figure 3. Linear regression for the ADM (-----), ILS (− − −). Ito (- - -) and ANA (….) with Gaussian pdf. The bisector (-. -.-.) was added as an eye guide

In order to perform a model validation we introduce an index κ which if identical zero there is a perfect match between the model and the experimental findings.

$$k = \sqrt{(a-1)^2 + \left(\frac{b}{\overline{C}_0}\right)^2} \quad \text{with} \quad \overline{C}_0 = \frac{1}{n}\sum_{i=1}^{n} C_{0i} \qquad (13)$$

Here a is the slope, b the intersection, C_{oi} the experimental data and $\overline{C}_0$ the arithmetic mean. Since both the experiment and the model are of stochastic character, fluctuations are present, but in the average model and experiment shall coincide, thus the introduced index represents a genuine model validation.

3.3. Solution for bi-Gaussian Turbulence

In the convective boundary layer, the heating of the air layer close to the ground produces turbulent flux which gives origin to the so-called up- and down-drafts.

This phenomenon is not symmetric but has a more intensive contribution from the up-drafts. Because of mass conservation the down-drafts occupy a larger area. As a consequence the stochastic term shall be asymmetric which excludes the Gaussian probability density as a convenient function. There is no indication for a unique probability density function so far, nevertheless the following characteristics shall be present.

• The probability density shall have an enhanced tail towards higher velocities, that indicate the more energetic up-drafts, but with a smaller integral proportion than down-drafts.

• The probability density shall have a pronounced maximum at negative velocities, i.e. the down-drafts.

One finds typically two types of asymmetric probability density functions in the literature, the bi-Gaussian and the Gram-Chalier distribution, where the latter is represented by a truncated series of Hermite polynomials.

In the further we discuss the bi-Gaussian probability density function, which contains a linear superposition of two Gaussian functions, one with maximum probability at a positive velocity, the other one at a negative value as for instance in ref.[7].The authors used a pair of Langevin equations, one for up- and one for down-drafts, each with its specific Gaussian function. In this work we condense this phenomenon in one equation, introducing a sum of two Gaussian functions with different parameters and relative weight.

$$P(z,w) = A_1 P_1(z,w) + A_2 P_2(z,w) \qquad (14)$$

where A_1 and A_2 define the relative proportions between up- (P_1) and down drafts (P_2) for the vertical turbulent velocities (w).

$$P(z,w) = \frac{1}{\sqrt{2\pi}}\frac{A_1}{\sigma_1}\exp\left[-\frac{1}{2}\left(\frac{w-m_1}{\sigma_1}\right)^2\right] + \frac{1}{\sqrt{2\pi}}\frac{A_2}{\sigma_2}\exp\left[-\frac{1}{2}\left(\frac{w-m_2}{\sigma_1}\right)^2\right] \qquad (15)$$

Here, m_1, m_2 are the average probabilities of P_1 and P_2, respectively, and σ_1 and σ_2 represent the standard deviations of each distribution. The mean up and down-draft velocities are

$$m_1 = \langle w_1 \rangle \quad \text{and} \quad m_2 = \langle w_2 \rangle \qquad (16)$$

and the respective standard deviations are

$$\sigma_1 = \left(\langle w_1^2 \rangle\right)^{\frac{1}{2}} \quad \text{and} \quad \sigma_2 = \left(\langle w_2^2 \rangle\right)^{\frac{1}{2}} \qquad (17)$$

A general prescription on how to determine the

parameters A_1, A_2, m_1, m_2, σ_1 and σ_2 consists in the usage of generating functionals of moments.

$$\langle w_n \rangle = \int_{-\infty}^{\infty} w_n P(z,w) dw \tag{18}$$

From the normalisation and the first four statistical moments one obtains an equation system which eliminates the unknowns.

$$A_1 + A_2 = 1 \tag{19}$$

$$A_1 m_1 + A_2 m_2 = 0 \tag{20}$$

$$A_1(m_1^2 + \sigma_1^2) + A_2(m_2^2 + \sigma_2^2) = \sigma_w^2 \tag{21}$$

$$A_1(m_1^3 + 3m_1\sigma_1^3) + A_2(m_2^3 + 3m_2\sigma_2^3) = \langle w^3 \rangle \tag{22}$$

$$A_1(m_1^4 + 6m_1^2\sigma_1^2 + 3\sigma_1^4) + A_2(m_2^4 + 6m_2^2\sigma_2^2 + 3\sigma_2^4) = \langle w^4 \rangle \tag{23}$$

Upon application of the bi-Gaussian probability density function the expression for the deterministic coefficient of the vertical dimension in the Langevin equation is then,

$$a_w = -w\frac{A_1P_1\sigma_1^2 + A_2P_2\sigma_2^2}{\sigma_1^2\sigma_2^2}\frac{C_0\varepsilon}{2P} + \left(\frac{A_1w_1P_1}{\sigma_1^2} + \frac{A_2w_2P_2}{\sigma_2^2}\right)\frac{C_0\varepsilon}{2P} + \frac{\phi}{P} \tag{24}$$

Using the deterministic coefficient the Langevin equation reads

$$\frac{dw}{dt} + \frac{A_1P_1\sigma_1^2 + A_2P_2\sigma_2^2}{\sigma_1^2\sigma_2^2}\frac{C_0\varepsilon}{2P}w = \left(\frac{A_1w_1P_1}{\sigma_1^2} + \frac{A_2w_2P_2}{\sigma_2^2}\right)\frac{C_0\varepsilon}{2P} + \frac{\phi}{P} + (C_0\varepsilon)^{\frac{1}{2}}\xi_w(t), \tag{25}$$

where ϕ is obtained upon application of the bi-Gaussian probability density function[36]:

$$\begin{aligned}\phi = &-\frac{1}{2}\left(A_1\frac{\partial w_1}{\partial z} + w_1\frac{\partial A_1}{\partial z}\right)erf\left(\frac{w-w_1}{\sqrt{2}\sigma_1}\right) \\ &+ w_1P_1\left[A_1\frac{\partial w_1}{\partial z}\left(\frac{w_2}{\sigma_1^2}+1\right) + w_1\frac{\partial A_1}{\partial z}\right] \\ &+ \frac{1}{2}\left(A_2\frac{\partial w_2}{\partial z} + w_2\frac{\partial A_2}{\partial z}\right)erf\left(\frac{w-w_2}{\sqrt{2}\sigma_2}\right) \\ &+ w_2P_2\left[A_2\frac{\partial w_2}{\partial z}\left(\frac{w^2}{\sigma_2^2}+1\right)w_2\frac{\partial A_2}{\partial z}\right]\end{aligned} \tag{26}$$

In a more compact form this yields for the Langevin equation with a bi-Gaussian probability density function (25)

$$\frac{dw}{dt} + \alpha_w w = \beta_w + \gamma_w + (C_0\varepsilon)^{\frac{1}{2}}\xi_w(t), \tag{27}$$

where

$$\begin{aligned}a_w &= \frac{A_1P_1\sigma_1^2 + A_2P_2\sigma_2^2}{\sigma_1^2\sigma_2^2}\frac{C_0\varepsilon}{2P}, \\ \beta_w &= \left(\frac{A_1w_1P_1}{\sigma_1^2} + \frac{A_2w_2P_2}{\sigma_2^2}\right)\frac{C_0\varepsilon}{2P}, \\ \gamma_w &= \frac{\phi}{P}\end{aligned} \tag{28}$$

Table 4. Comparison of the linear regressions of ADM, ILS, Ito and ANA for a Gaussian pdf

Modelo	Regression	R^2	K
ADM	y = 0.93x + 23.50	0.89	0.07
ILS	y = 1.04x + 105.51	0.87	0.09
Ito	y = 0.70x + 296.13	0.83	0.37
ANA	y = 0.62x + 552.32	0.33	0.56

In Table (5) the concentrations of the measurements together with theoretical predictions of ADM, ILS and Ito are presented. Table (6) shows the numerical convergence of the ADM method. As already evident in the previous case also for the bi-Gaussian probability density function only a few terms are necessary in order to represent a solution.

Figure (5) shows the dispersion plot of the experimental values against the theoretical predicted values by ADM, ILS and the Ito calculus.

We also apply the model validation as introduced in the previous section to the model application with the bi-Gaussian probability density function. One observes that the all three approaches are more or less close to the bisector, however the comparison with the model validation from the previous case shows that the Gaussian probability density function seems more adequate for the stability condition of the experiment which is also manifest in the smallest k for ADM.

From the comparison of the regressions in table 7 one recognizes that the three approaches behave similar with respect to R^2 but show larger values for k in comparison to the case where the Gaussian probability density function defined the stochastic character of the turbulence.

Table 5. Concentrations from Copenhagen experiment and prediction from ADM, ILS, Ito using a bi-Gaussian pdf

Exp.	Distance (m)	Observed (μgm^{-2})	Predictions Cy (μgm^{-2})		
			ADM	ILS	Ito
1	1900	2074	2001	1976	1901
1	3700	739	1115	1073	1027
2	2100	1722	1335	1547	1196
2	4200	944	713	1415	799
3	1900	2624	2672	3020	2629
3	3700	1990	1586	1871	1499
3	5400	1376	1129	1399	1116
4	4000	2682	2194	3001	1877
5	2100	2150	2464	2231	2378
5	4200	1869	1646	1945	1758
5	6100	1590	1377	1823	1549
6	2000	1228	1020	1044	936
6	4200	688	476	545	571
6	5900	567	322	552	486
7	2000	1608	1104	1584	1021
7	4100	780	472	1175	704
7	5300	535	357	1072	442
8	1900	1248	1293	1302	1118
8	3600	606	649	943	700
8	5300	456	427	610	532
9	2100	1511	1421	1669	1256
9	4200	1026	708	1543	797
9	6000	855	503	1051	600

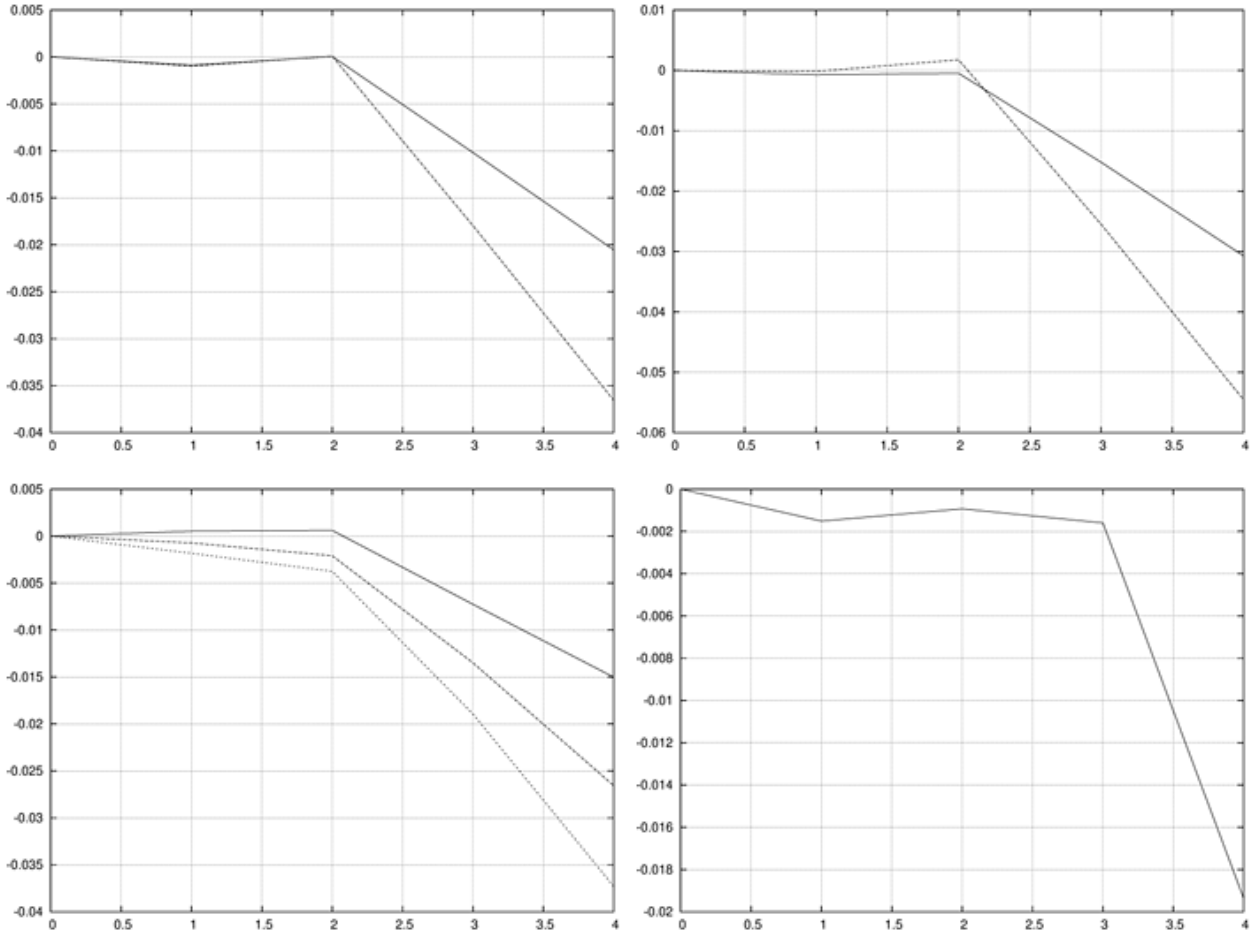

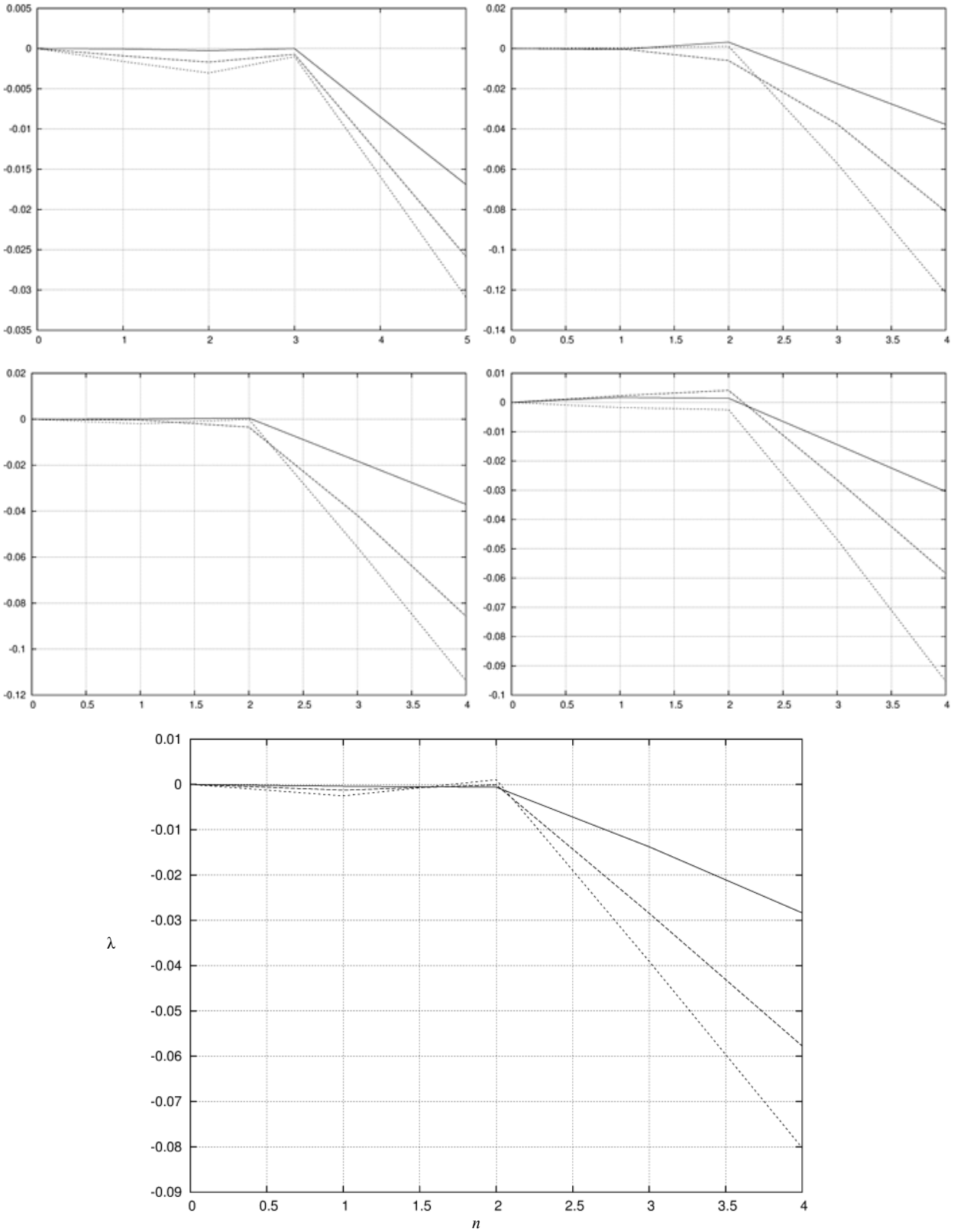

Figure 4. Lyapunov exponent λ of the Adomian approach depending on the number *n* of terms for the 9 experimental runs using the bi-Gaussian pdf.

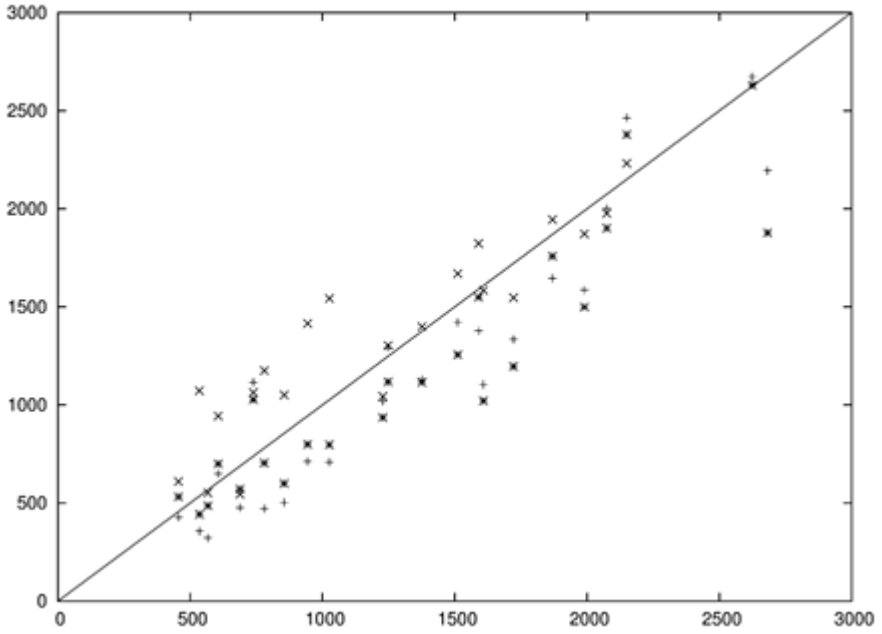

Figure 5. Dispersion diagram of predicted (Cp) measured against measured (Co) values by by ADM (+), ILS (×) and Ito (*) for a bi-Gaussian pdf

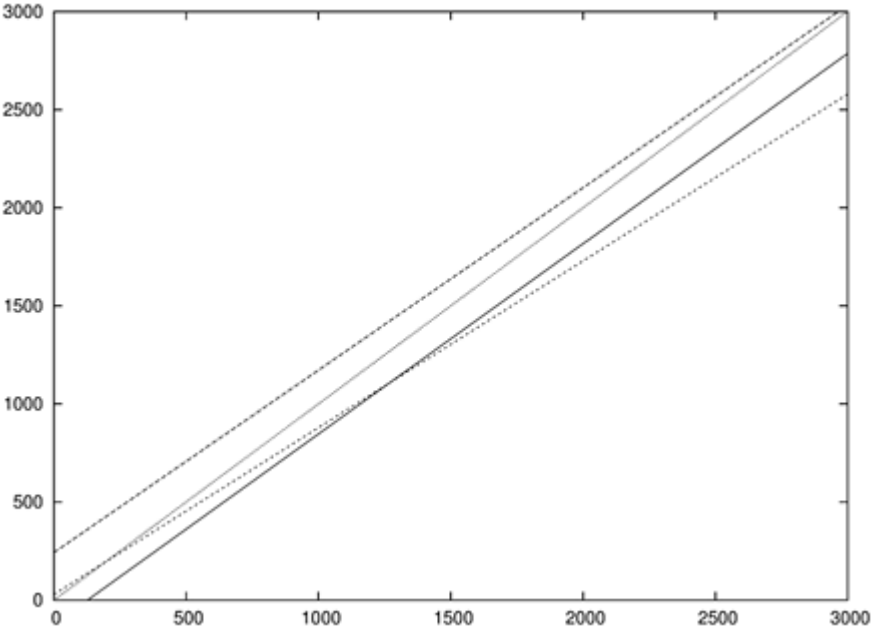

Figure 6. Linear regression for the ADM (——), ILS (– – –) and Ito (- - - -) with a Bi-Gaussian pdf. The bisector (– · – ·) was added as an eye guide

Table 6. Numerical convergence of ADM for a bi-Guassian pdf . The multiple columns for *Cy* refer to the measurements at different distances per run and are given in table 5

Run	Terms	Cy (μgm-2)		
1	u0	1930,605	1164.849	
	u0 + u1	1988.625	1097.584	
	u0 + u1 + u2	1923.805	1169.695	
	u0 + u1 + u2 + u3	2000.73	1114.916	
	u0 + u1 + u2 + u3 + u4	2000.73	1114,916	
2	u0	1268,718	705.3707	
	u0 + u1	1310.076	706.2147	
	u0 + u1 + u2	1299.548	687.1277	
	u0 + u1 + u2 + u3	1335.249	713.1350	
	u0 + u1 + u2 + u3 + u4	1335.249	713.1350	
3	u0	2645.291	1388.329	934.7424
	u0 + u1	2569.380	1520.158	1152.943
	u0 + u1 + u2	2545.731	1592.848	1132.120
	u0 + u1 + u2 + u3	2671.856	1585.870	1129.320
	u0 + u1 + u2 + u3 + u4	2671.856	1585.870	1129.320
4	u0	1918.952		
	u0 + u1	2183.475		
	u0 + u1 + u2	2156.671		
	u0 + u1 + u2 + u3	2201.707		
	u0 + u1 + u2 + u3 + u4	2193.560		
5	u0	2342.774	1341.859	1061.910
	u0 + u1	2573.369	1572.562	1340.005
	u0 + u1 + u2	2527.639	1664.515	1371.924
	u0 + u1 + u2 + u3	2585.538	1545.632	1290.100
	u0 + u1 + u2 + u3 + u4	2464.081	1646.118	1376.838
		2464.081	1646.118	1376.838
6	u0	1024.609	470.6826	312.2561
	u0 + u1	1016.280	481.9288	311.2449
	u0 + u1 + u2	925.6591	476.7062	308.4274
	u0 + u1 + u2 + u3	1019.558	476.3795	321.7595
	u0 + u1 + u2 + u3 + u4	1019.558	476.3795	321.7595
7	u0	1048.864	510.2945	401.3791
	u0 + u1	1042.545	439.8970	378.0348
	u0 + u1 + u2	1012.276	479.4384	400.1880
	u0 + u1 + u2 + u3	1104.080	472.1360	357.2161
	u0 + u1 + u2 + u3 + u4	1104.080	472.1360	357.2161
8	u0	1280.617	646.3909	378.3521
	u0 + u1	1193.205	662.8212	402.9780
	u0 + u1 + u2	1219.809	702.0541	443.7521
	u0 + u1 + u2 + u3	1293.085	649.3011	427.3928
	u0 + u1 + u2 + u3 + u4	1293.085	649.3011	427.3928
9	u0	1452.223	652.5918	469.1815
	u0 + u1	1438.980	729.6335	493.3640
	u0 + u1 + u2	1433.919	656.2526	448.3562
	u0 + u1 + u2 + u3	1420.842	707.7180	503.2054
	u0 + u1 + u2 + u3 + u4	1420.842	707.7180	503.2054

Table 7. Comparison of the linear regressions using the bi-Gaussian probability density function

Model	Regression	R^2	K
ADM	y = 0.97x -123.47	0.89	0.10
ILS	y = 0.93x +242.34	0.89	0.19
Ito	y = 0.85x +29.07	0.86	0.15

3.4. Solution for Gram-Chalier Turbulence

The use of the Gram-Chalier probability density function for stochastic Lagrangian models was proposed by Ferrero and Anfossi (1998)[23] (see also the work by Jensen et al. (1997)[33]), which makes use of an expansion in Hermite polynomials. In the present discussion we use the series until the fourth term resulting in an asymmetric probability density function for the vertical turbulent velocities.

$$P(r,z)=\frac{e^{-\frac{r^2}{2}}}{\sqrt{2\pi}}\left(1+c_3H_3+c_4H_4\right), \qquad (29)$$

Table 8. Concentration of the Copenhagen experiment in comparison to the predictions by ADM, ILS and Ito using a Gram-Chalier pdf

Exp.	Distance (m)	Observation (μgm^{-2})	Prediction (μgm^{-2})		
			ADM	ILS	Ito
1	1900	2074	1957	1721	2698
1	3700	739	976	761	1956
2	2100	1722	1256	1273	1222
2	4200	944	754	928	944
3	1900	2624	3426	2612	2689
3	3700	1990	1680	2069	2198
3	5400	1376	1178	1064	1591
4	4000	2682	2940	2754	2072
5	2100	2150	2855	2499	1717
5	4200	1869	1430	1658	1742
5	6100	1590	1136	1432	1553
6	2000	1228	1244	995	712
6	4200	688	797	618	690
6	5900	567	573	537	558
7	2000	1608	1490	1201	1398
7	4100	780	707	863	993
7	5300	535	628	723	836
8	1900	1248	1074	1170	1178
8	3600	606	690	728	694
8	5300	456	495	604	653
9	2100	1511	1672	1550	1246
9	4200	1026	993	1450	1112
9	6000	855	932	1281	983

where

$$c_3=\frac{1}{6}\mu_3, c_4=\frac{1}{24}\left(\mu_4-6\mu_2+3\right), \qquad (30)$$

$$H_3=r^3-3r, H_4=r^4-6r^2+3 \qquad (31)$$

and $r=\frac{u_i}{\sigma_i}$. In the case of Gaussian turbulence equation (29) recovers the normal distribution with c_3 and c_4 equal zero. The Gram-Charlier probability density function of the third order is obtained by the choice $c_4 = 0$. Upon application of equation (29) in the equation of the deterministic coefficients yields,

$$a(x_i,u_i)=\frac{f_i}{h_i}\frac{\sigma_i}{\tau_{Li}}+\sigma_i\frac{\sigma_i}{x_j}\frac{g_i}{h_i}, \qquad (32)$$

where $j = 1, 2, 3$ and $j \neq i, \tau_{Li}$ is the Lagrangian correlation time scale and f_i, g_i and h_i are expressions as shown below.

$$f_i = -3C_3 - r_i(15C_4 + 1) + 6C_3 r_i^2 + 10C_4 r_i^3 + - C_3 r_i^4 - C_4 r_i^5 \quad (33)$$

$$g_i = 1 - C_4 - r_i^2(1 + C_4) - 2C_3 r_i^3 + - 5C_4 r_i^4 + C_3 r_i^5 + C_4 r_i^6 \quad (34)$$

$$h_i = 1 - 3C_4 - 3C_4 r_i - 6C_4 r_i^2 + C_3 r_i^3 + C_4 r_i^4 \quad (35)$$

Inserting the deterministic coefficient (32) into the Langevin equation renders the latter

$$\frac{du_i}{dt} = \frac{f_i}{g_i}\frac{\sigma_i}{\tau_{Li}} + \sigma_i \frac{\partial \sigma_i}{\partial x_j}\frac{g_i}{h_i} + (C_o \varepsilon)^{\frac{1}{2}} \xi_i(t). \quad (36)$$

Table 9. Numerical convergence of ADM using a Gram-Chalier pdf. The multiple columns for C_y refer to the measurements at different distances per run and are given in table 8

Run	Terms	*Cy* (μgm^{-2})		
1	u_0	2134.374	905.1679	
	$u_0 + u_1$	1958.222	975.6816	
	$u_0 + u_1 + u_2$	1957.265	976.3862	
	$u_0 + u_1 + u_2 + u_3$	1957.265	976.3862	
2	u_0	1215.582	733.3223	
	$u_0 + u_1$	1258.735	683.5825	
	$u_0 + u_1 + u_2$	1256.363	754.4139	
	$u_0 + u_1 + u_2 + u_3$	1256.363	754.4139	
3	u_0	3431.128	1602.438	1114.993
	$u_0 + u_1$	3422.063	1700.270	1165.802
	$u_0 + u_1 + u_2$	3425.766	1679.948	1177.613
	$u_0 + u_1 + u_2 + u_3$	3425.766	1679.948	1177.613
4	u_0	3066.27		
	$u_0 + u_1$	2911.51		
	$u_0 + u_1 + u_2$	2939.85		
	$u_0 + u_1 + u_2 + u_3$	2939.85		
5	u_0	2817.202	1396.448	1075.217
	$u_0 + u_1$	2858.730	1434.506	1134.203
	$u_0 + u_1 + u_2$	2855.275	1429.748	1136.310
	$u_0 + u_1 + u_2 + u_3$	2855.275	1429.748	1136.310
6	u_0	1273.45	851.0902	525.1321
	$u_0 + u_1$	1304.966	797.4598	559.2511
	$u_0 + u_1 + u_2$	1243.54	797.4534	572.6406
	$u_0 + u_1 + u_2 + u_3$	1243.54	797.4534	572.6406
7	u_0	1461.67	672.4225	613.2297
	$u_0 + u_1$	1868.749	699.8157	631.2928
	$u_0 + u_1 + u_2$	1489.976	707.4423	627.6641
	$u_0 + u_1 + u_2 + u_3$	1489.976	707.4423	627.6641
8	u_0	973.0740	691.4625	512.5447
	$u_0 + u_1$	1074.354	702.0862	497.4521
	$u_0 + u_1 + u_2$	1073.538	690.2837	494.8708
	$u_0 + u_1 + u_2 + u_3$	1073.538	690.2837	494.8708
9	u_0	1647.435	1054.789	898.2956
	$u_0 + u_1$	1662.513	963.0107	883.1010
	$u_0 + u_1 + u_2$	1671.778	992.9380	936.4106
	$u_0 + u_1 + u_2 + u_3$	1671.788	992.9380	932.4106
	$u_0 + u_1 + u_2 + u_3 + u_4$	1671.788	992.9380	932.4106

In short hand notation this reads

$$\frac{du_i}{dt} = \alpha_i + \beta_i + (C_0 \varepsilon)^{\frac{1}{2}} \xi_i(t), \quad (37)$$

where

$$\alpha_i = \frac{f_i}{g_i}\frac{\sigma_i}{\tau_{Li}}, \quad (38)$$

$$\beta_i = \sigma_i \frac{\partial \sigma_i}{\partial x_j}\frac{g_i}{h_i}. \quad (39)$$

In table (8) we present the concentrations of the Copenhagen experiment together with the results from the ADM, ILS and Ito approaches.

Table 9 shows the numerical convergence of the ADM method. As in the two previous cases only a few terms reproduce with considerable fidelity the exact solution with a Gram-Chalier probability density function.

Figure (8) shows the dispersion plot of observed against predicted data. In Figure (9) are shown the linear regression for the three approaches. All three methods, ADM, ILS and Ito reproduce reasonably well the expected bisector. Using the model validation index k shows that for all three probability density functions the ADM approach yields results closest to the expected concentration profile.

As already mentioned before, the model validation indicates the Gaussian probability density function implemented together with the ADM approach as the most adequate description for the Copenhagen experiment by virtue of $k = 0.07$ being significantly smaller than all other realizations. This was also to be expected from the stability conditions given in table 10, which characterize the turbulence regime as strong convective.

Table 10. Comparison of the linear regressions for the ADM, ILS and Ito approach using the Gram-Chalier probability density function

Model	Regression	R^2	k
ADM	y = 1.09x + 113,83	0.85	0.12
ILS	y = 0.90x + 112.17	0.87	0.13
Ito	y = 0.78x +324.52	0.62	0.33

It is worth mentioning that since convergence is genuinely controlled the present procedure permits to pin down model limitations which in other approaches are hidden in numerical imprecision or approximations.

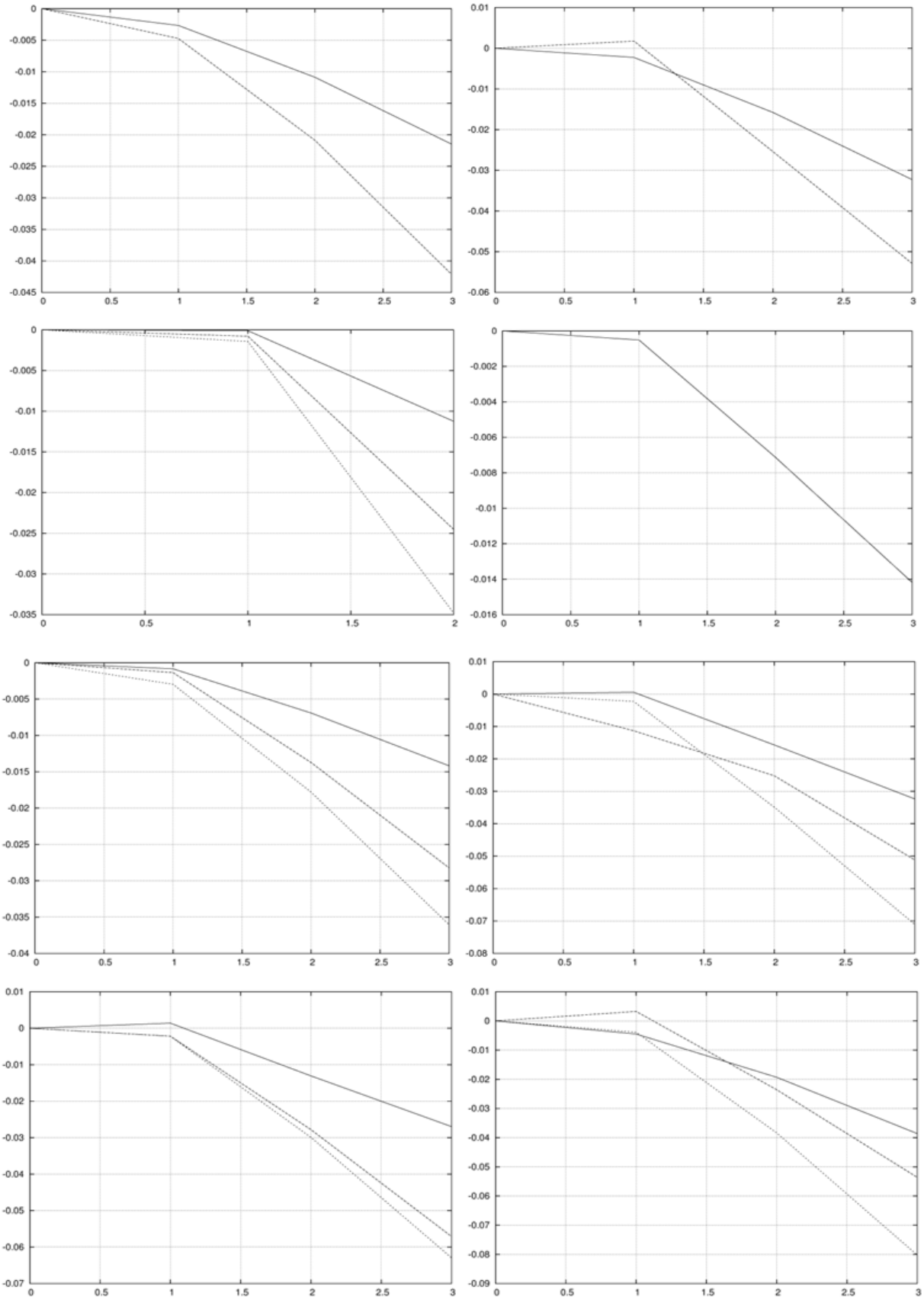

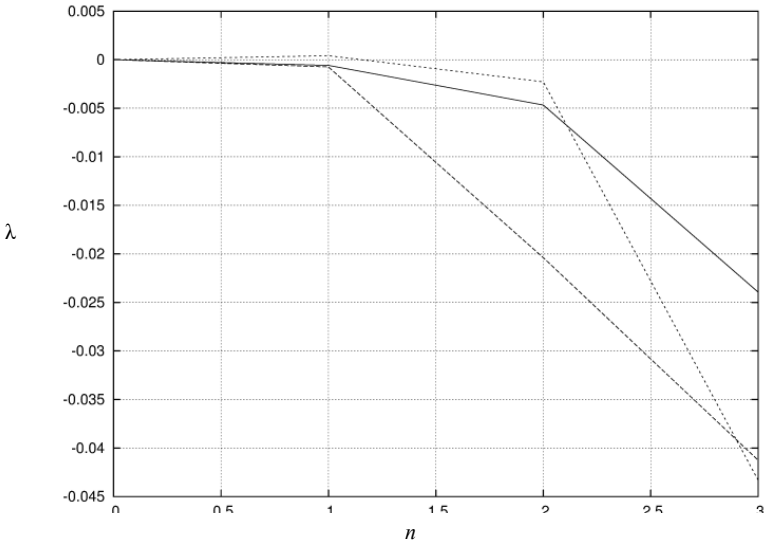

Figure 7. Lyapunov exponent λ of the Adomian approach depending on the number of terms n for the 9 experimental runs using the Gram-Chalier pdf

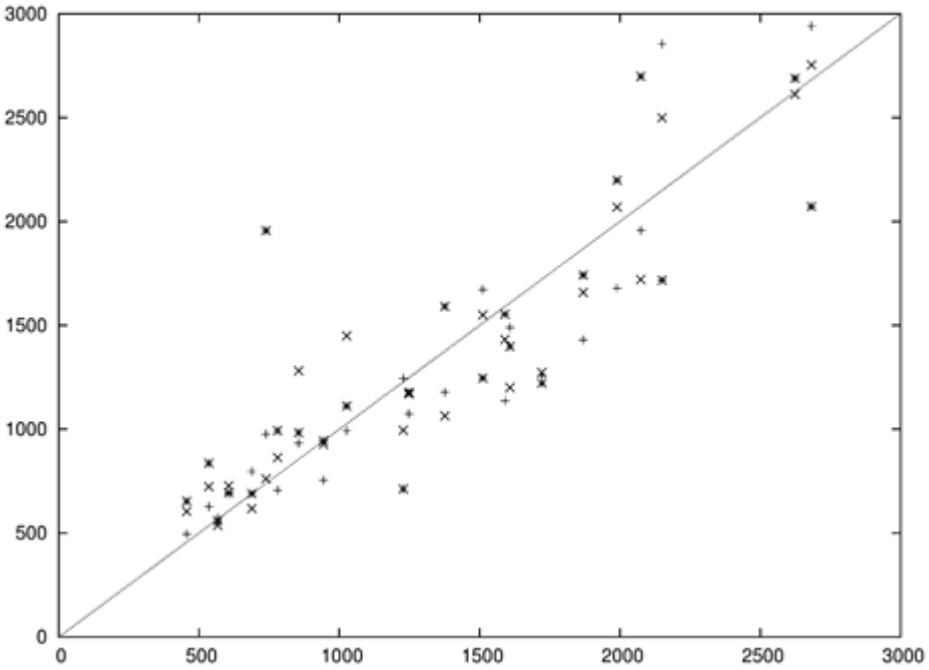

Figure 8. Dispersion diagram of predicted (C_p) against observed values (C_o) with a Gram-Chalier probability density function

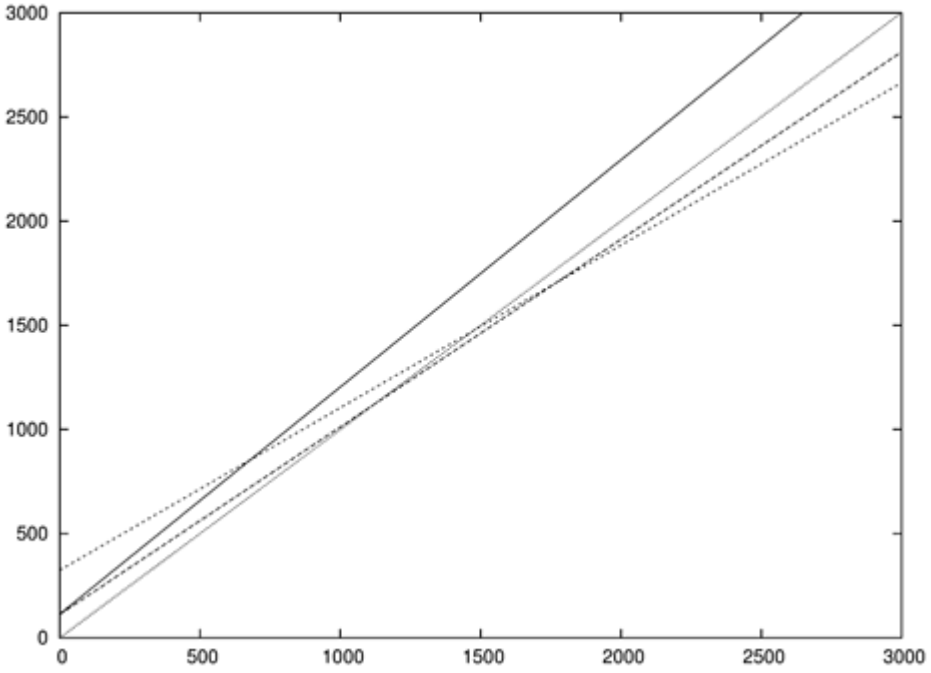

Figure 9. Linear regression using the Gram-Chalier probability density function

4. Conclusions

In the present contribution we discussed an approach that is designed to simulate meteorological aspects, that are relevant in eolic park site evaluation. We showed how a realiable model for a turbulent wind profile may be determined among model candidates, that provides the full three dimensional space and time dependent turbulent wind field for an area in consideration.

We showed in a general form how to construct a recursive scheme where convergence is understood. A genuine criterion was introduced based on Lyapunov's theory, that in our case tests stability of convergence. Application of that criterion showed that in all three cases only five terms are necessary so that the approximate solution differs from the real solution by less than one percent.

On the one hand, the generality of the proposed solution with respect to the considered probability density functions on the other hand the controlled convergence permits to validate the model in question. The resulting model is thus likely to simulate turbulent wind profiles close to those that could be observed in a site in question.

The Gaussian density function yields within the phenomenon inherent fluctuations the best agreement between model and observation. Among the three probability distributions the Gaussian one is from the physics point of view considered the most adequate for the Copenhagen experiment. Thus the criterion to select a model among possible candidates identified the most adequate one.

We believe that we have done a step into a new direction with the present contribution, that may be useful to analyse meteorological aspects as well as simulate possible scenarios, for the purpose of site evaluation, using tracer experiments. Since measurements are typically performed in a limited set of positions a calibrated model is able to reconstruct the three dimensional wind velocity field considering especially the contributions by turbulence. To the best of our knowledge up-to-date the tracer technique is not used for site evaluation, but could supply valuable information on the wind properties for a given region of interest and its time-behaviour.

In this paper we presented an analytical solution of the three-dimensional stochastic Langevin equatioqn applied to tracer dispersion for Gaussian, bi-Gaussian and Gram-Chalier turbulence, respectively. The solution was obtained using the Adomian Decomposition Method (ADM) whose principal advantage relies in the fact that the non-linearity can be taken care of without linearisation or simplifications. Further, the stochastic part is absorbed in the initial term of the iteration and thus propagates through all the subsequent iteration terms. For the Langevin equation the non-trivial questions of uniqueness and convergence for the Adomian approach in stochastic problems is given since the drift and dispersion terms satisfy a Lipschitz condition.

REFERENCES

[1] Adomian, G. "A Review of the Decomposition Method in Applied Mathematics", J. Math. Anal. Appl., vol. 135, pp. 501-544, 1988.

[2] Adomian, G. Solving Frontier Problems of Physics: The Decomposition Method, Kluwer, USA, 1994.

[3] Adomian, G. "Solution of coupled non-linear partial differential equations by decomposition", Comp. Math. Appl.,

vol. 31, pp. 117-120, 1996.

[4] Aminataei, A., Hosseini, S.S. Applied Mathematics and Computation , vol. 1, pp. 665-669, 2007.

[5] Arya, S.P. Air Pollution Meteorology and Dispersion, Oxford University Press, USA, 1999.

[6] Arya, S.P. "A review of the theoretical bases of short-range atmospheric dispersion and air quality models", , Proc. Indian Natn. Sci. Acad., vol. 69A, pp. 709-724, 2003.

[7] Baerentsen, J.H., Berkowicz, R. "Monte-Carlo Simulation of Plume Diffusion in the Convective Boundary Layer", Atmos. Environ, vol. 18, pp. 701-712, 1984.

[8] Brebbia, C.A. Progress in Boundary Element Methods, Pentech Press, London, 1981.

[9] Boichenko, V.A., Leonov, G.A., Reitmann, V. Dimension theory for ordinary equations, Teubner, Stuttgart, 2005.

[10] Burden, R.L. Numerical analysis. 8th ed., Thomson-Brooks/Cole, Belmont, CA, 2005.

[11] Calaf, M., Meneveau, C., Meyers, J. "Large eddy simulation study of fully developed wind-turbine array boundary layers", Phys. Fluids, vol. 22, pp. 015-110, 2010.

[12] Carvalho, J.C., Vilhena, M.T. "Pollutant dispersion simulation for low wind speed condition by the ILS method", Atmos. Environm., vol. 39, pp. 6282-6288, 2005.

[13] Carvalho, J.C., Nichimura, E.R. Vilhena, M.T., Moreira, D.M., Degrazia, G.A. "An iterative langevin solution for contaminant dispersion simulation using the Gram-Charlier PDF", Environm. Mod. And Soft., vol. 20, pp. 285-289, 2005.

[14] Carvalho, J.C., Vilhena, M.T., Moreira, D.M. "An alternative numerical approach to solve the Langevin equation applied to air pollution dispersion", Water Air and Soil Pollution, vol. 163, pp. 103-118, 2005.

[15] Carvalho, J.C., Vilhena, M.T., Thomson, M. "An iterative Langevin solution for turbulent dispersion in the atmosphere", J. Comp. Appl. Math., vol. 206, pp. 534-548, 2007.

[16] Carvalho, J.C., Vilhena, M.T., Moreira, D.M. "Comparison between Eulerian and Lagrangian semi-analytical models to simulate the pollutant dispersion in the PBL". Appl. Math. Model., vol. 31, pp. 120-129, 2007.

[17] Chock, D.P., Sun, P.,Winkler, S.L. "Trajectory-grid: an accurate sign preserving advection-diffusion approach for air quality modeling", Atmos. Environ., vol. 30, no. 6, pp. 857-868, 1996.

[18] Degrazia, G.A., Anfossi, D., Carvalho, J.C., Mangia, C., Tirabassi, T., Campos Velho, H.F. "Turbulence parameterization for PBL dispersion models in all stability conditions", Atmos. Environ., vol. 34, pp. 3575-3583, 2000.

[19] Dehghan, M. "The use of Adomian decomposition method for solving the one dimensional parabolic equation with non-local boundary specification", Int. J. Comput. Math., vol. 81, pp. 25-34, 2004.

[20] Dike, M.V. Perturbation Methods in Fluid Mechanics, Academic Press, USA, 1975.

[21] El-Wakil, S.A., Elhanbaly, A., Abdou, M.A. "Adomian decomposition method for solving fractional non-linear differential equations", Appl. Math. Comput., vol.182, no.1, pp. 313-324, 2006.

[22] Eugene, Y. "Application of the decomposition to the solution of the reaction-convection-diffusion equation", Appl. Math. Comput. vol. 56, pp. 1-27, 1993.

[23] Ferrero, E., Anfossi, D., Tinarelli, G., Tamiazzo, M.. "Inter-comparison of Lagrangian stochastic models based on two different PDFs", International Journal of Environment and Pollution, vol.14, pp. 225-234, 2000

[24] Gardiner, C.W. Handbook of stochastic methods for physics, chemistry and the natural sciences, Springer-Verlag, Germany, 1985.

[25] Grisogono, B., Oerlemans, J. "Katabatic flow: analytic solution for gradually varying eddy diffusivities", J. Atmos. Sci., vol. 58, pp. 3349-3354, 2001.

[26] Gryning, S.E., Lyck, E. "Atmospheric dispersion from elevated source in un urban area: comparison between tracer experiments and model calculations", J. Climate Appl. Meteor., vol. 23, pp. 651-654, 1984.

[27] Gryning, S.-E., Batchvarova, E., Br¨ummer, B., Jørgensen, H., Larsen, S. "On the extension of the wind profile over homogeneous terrain beyond the surface boundary layer". Boundary-Layer Meteorol., vol. 124, pp. 251-268, 2007.

[28] Hanna, S.R. "Confidence limit for air quality models as estimated by bootstrap and jackknife re-sampling methods", Atmos. Environm. vol. 23, pp. 1385- 1395, 1989.

[29] Henry, R.C., Wand, Y.J., Gebhart, K.A. "The relationship between empirical orthogonal functions and sources of air pollution", Atmos. Environ., vol.25A, pp. 503-509, 1991.

[30] Hinze, J.O. Turbulence. Mc Graw Hill, vol. 1, CRC Press, Inc., USA, 1986.

[31] Huebner, K.H.H., Dewhirst, D.L., Smith, D.E., Byrom, T.G. Finite Element Method for Engineers, J. Wiley & Sons, USA, 2001.

[32] Inc, M. "On numerical solutions of partial differential equations by the decomposition method", Kragujevac J. Math. vol. 26, pp. 153-164, 2004.

[33] Jensen, A.K.V, Gryning, S.E. "A new formulation of the probability density function in a random walk model for atmospheric dispersion". Air Pollution Modelling and its Application XII, Plenum Press, USA, pp. 429-438, 1997.

[34] Laffer, P., Abbaoui, K. "Modelling of the thermic exchanges during a drilling. resolution with Adomian's decomposition method", Math. and Comp. Model. vol. 23, no. 10, pp. 11-14, 1996.

[35] Lin, J.S., Hildemann, L.M. "Analytical solutions of the atmospheric diffusion equation with multiple sources and height-dependent wind speed and eddy diffusivities", Atmos. Environ. vol. 30, pp. 239-254, 1997.

[36] Luhar, A.K., Hibberd, M.F., Hurley, P.J. "Comparison of Closure Schemes Used to Specify the Lagrangian Stochastic Dispersion Models for Convective Conditions", Atmos. Environ. vol. 30, pp. 1407-1418, 1996.

[37] Metha, K.N., Yadav, A.K. Indian J. Pure and Appl. Math., vol. 34, pp. 963-974, 2003.

[38] Meyers, J., Meneveau, C. "Optimal turbine spacing in fully developed wind farm boundary layers", Wind Energy (online: 14 APR 2011), DOI: 10.1002/we.469, 2011.

[39] Parlange, J.Y. "Theory of water movement in soils: I. One-dimensional absorption", Soil Sci., vol. 111, no. 2, pp. 134-137, 1971.

[40] Rodean, H.C. Stochastic Lagrangian models of turbulent diffusion, American Meteorological Society, USA, 1996.

[41] Sharan, M., Kansa, E.J., Gupta, S. "Application of the multi-quadric method for numerical solution of elliptic partial differential equations", Applied Mathematics and Computation, vol. 84, pp. 275-302, 1997.

[42] Seinfeld, J.H., Pandis, S.N. Atmospheric Chemistry and Physics, J. Wiley & Sons, USA.

[43] Sharan, M., Manish, M., Yadav, K. "Atmospheric dispersion: an overview of mathematical modelling framework", Proc. Indian Nat. Sci. Acad. vol. 69A, no. 6, pp. 725-744, 2003.

[44] Szinvelski, C.R.P., Vilhena, M.T.M.B., Carvalho, J.C., Degrazia, G.A. "Semi-analytical solution of the asymptotic langevin equation by the Picard iterative method", Environm. Mod. And Soft. vol. 21, no. 3, pp. 406-410, 2006.

[45] Tangerman, G. "Numerical simulations of air pollutant dispersion in a stratified planetary boundary layer", Atmos. Environ. vol. 12, pp. 1365-1369, 1978.

[46] Tennekes, H. Similarity relation, scaling laws and spectral dynamics, in: F.T.M. Nieuwstadt and H. Van Dop (Eds.), Atmospheric Turbulence and Air Pollution Modelling, Reidel, Dordrecht, pp. 37-68, 1982.

[47] Uhlenbeck, G.E., Ornstein, L.S. "On the theory of the Brownian motion", Phys. Rev., vol. 36, pp. 823-841, 1930.

[48] Zannetti, P. Air Pollution Modelling, Southampton, Comp. Mech. Publications, UK, 1990.